Section 3 Optics and Devices

Chapter 1. Optics and Quantum Electronics

Academic and Research Staff

Professor Hermann A. Haus, Professor Erich P. Ippen, Professor James G. Fujimoto, Professor Peter L. Hagelstein, Dr. Santanu Basu, Dr. Joseph A. Izatt

Visiting Scientists and Research Affiliates

Dr. Lucio H. Acioli, Yuzo Hirayama, Dr. Franz X. Kärtner, Dr. Charles P. Lin, Dr. Antonio Mecozzi, Dr. Jeróme M. Paye, Dr. Masataka Shirasaki, Dr. Fabrice Vallee

Graduate Students

Laura E. Adams, Keren Bergman, Luc Boivin, Jeffrey K. Bounds, Tak K. Cheng, Ali Darwish, Jay N. Damask, Ali M. Darwish, Christopher R. Doerr, David J. Dougherty, Siegfried B. Fleischer, James G. Goodberlet, Katherine L. Hall, Michael R. Hee, David Huang, Charles T. Hultgren, Joseph M. Jacobson, Sumanth Kaushik, Farzana I. Khatri, Gadi Lenz, Ilya Lyubomirsky, Martin H. Muendel, John D. Moores, Ann W. Morgenthaler, Lynn E. Nelson, Janet L. Pan, Lily Y. Pang, Malini Ramaswamy, Chi-Kuang Sun, Kohichi R. Tamura, Morrison Ulman

Undergraduate Students

Irfan U. Chaudhary, Darlene J. Ford, Akikazu Hashimoto, Jalil Kahn

Technical and Support Staff

Mary C. Aldridge, Donna L. Gale, Cynthia Y. Kopf, Lisbeth N. Lauritzen

1.1 Additive Pulse Modelocking

Sponsors

Joint Services Electronics Program
Contract DAAL03-92-C-0001
U.S. Air Force - Office of Scientific Research
Contract F49620-91-C-0091

Project Staff

Professor James G. Fujimoto, Professor Hermann A. Haus, Professor Erich P. Ippen, Dr. Antonio Mecozzi, Farzana I. Khatri, John D. Moores, Lynn E. Nelson

Additive Pulse Modelocking (APM) is a technique of modelocking that simulates saturable absorber action by transforming nonlinear phase modulation due to the Kerr effect into amplitude modulation. Since the Kerr effect has a very short response time, very fast absorption characteristics can be achieved. The Kerr effect is also responsible for self-focusing, an effect used in the Kerr Lens Modelocking (KLM).

In order to compare the two modelocking schemes, we have developed an analytic theory of KLM.[1] With the analytic theory of APM already available, it was possible to make comparisons on the merits of the two schemes.[1]

It has been observed by several researchers that achievable pulsewidths are critically dependent upon third order dispersion of the system (the dependence of the group velocity dispersion upon frequency). We have gained a good understanding of the process by extensive computer simulations and an analytic treatment that is capable of reproducing the main features of the simulation results.[2] Briefly stated, third order dispersion generates sidebands of the pulse spectrum because the dispersion characteristic provides phase matching of the main pulse phase velocity with the phase velocity of a spectral sideband of the pulse. This effect drains energy from the main pulse and

---

[1] H.A. Haus, J.G. Fujimoto, and E.P. Ippen, "Analytic Theory of Additive Pulse and Kerr Lens Mode Locking," *IEEE J. Quant. Electron.* 28: 2086-2096 (1992).

[2] H.A. Haus, J.D. Moores, and L.E. Nelson, "Effect of Third-order Dispersion on Passive Mode Locking," *Opt. Lett.* 18: 51-53 (1993).

reduces the saturable absorber action. A surprising outcome of the analysis is that, when third order dispersion effects are significant, the pulse can be shortened by filtering its spectrum. This filtering reduces the sideband generation and thus reduces its damaging effect.

Another theoretical investigation was triggered by observations of C. Doerr, a graduate student attempting to actively modelock an erbium fiber ring laser to produce high repetition rate pulse trains. It was hoped that the relatively short solitons (1 ps or less) in the laser with negative group velocity dispersion could be forced to circulate at a Gbit rate. Mr. Doerr found that he could achieve good steady state pulse generation with 100 ps pulses, but not shorter ones. The computer simulations made by L. Nelson, aided by analytic work, showed that this is consistent with theoretical predictions. The modelocked pulses can be shortened somewhat by the Kerr effect in the fiber, as already pointed out in our previous work.[3] However, when much shorter pulses are attempted with increased Kerr effect, the system is forced to produce pulses closely resembling higher order solitons. These pulses, of course, change continuously and cannot lead to a steady state pulse train of constant amplitude. This work also provides a good physical interpretation for Haus and Silberberg,[3] which did not provide a physical explanation of the results of its computer simulations. It is clear, however, that both very short pulses and pulse timing via active modelocking are achievable when APM components are introduced into the laser system. We shall pursue this problem both theoretically and experimentally.

1.2 Fiber Ring Laser

Sponsors

Charles S. Draper Laboratories
Contract DL-H-441629
Joint Services Electronics Program
Contract DAAL03-92-C-0001
U.S. Air Force - Office of Scientific Research
Contract F49620-91-C-0091

Project Staff

Professor Hermann A. Haus, Professor Erich P. Ippen, Christopher R. Doerr, Lynn E. Nelson, Kohichi R. Tamura

Work on all-fiber modelocked lasers is being pursued at several laboratories, e.g., the Naval Research Laboratory and the University of Southampton. We have concentrated on one particular realization, a simple unidirectional additively pulse modelocked (APM) ring erbium fiber laser. The gain fiber also acts as the nonlinear Kerr element. Fiber polarization transformers and fiber polarizer and isolator make this an all-fiber system.

K. Tamura was successful in obtaining stable operation of the laser[4] with pulses at 42 MHz repetiton rate (one pulse in the ring) of 452 fs duration. The system is truly self-starting because it breaks into pulse operation spontaneously when a 36 mw pump threshold is reached (cw operation is initiated at 11 mw pump power). The self-starting behavior is in agreement with our previously published theory[5] that showed self-starting impeded by small backscatter in the laser resonator. The scatter displaces the resonator mode spectrum and thereby calls for increased injection signals into the individual modes. In the unidirectional ring only a combination of two backscatters (one backward, the other forward) displaces the resonator mode spectrum, and hence the effect is greatly reduced.

The very successful operation of this laser has encouraged us to intensify the work on this particular system. We will implement schemes to obtain stable operation with more than one pulse within the resonator, and we will work toward generation of even shorter pulses.

1.3 Long Distance Fiber Communications

Sponsors

MIT Lincoln Laboratory
National Science Foundation
Grant ECS 90-12787

---

3 H.A. Haus and Y. Silberberg, "Laser Mode Locking with Addition of Nonlinear Index," *IEEE J. Quant. Electron.* QE-22: 325-331 (1986).

4 K. Tamura, H.A. Haus, and E.P. Ippen, "Self-starting Additive Pulse Mode-locked Erbium Fibre Ring Laser," *Electron. Lett.* 28: 2226-2227 (1992).

5 H.A. Haus and E.P. Ippen, "Self-starting of Passively Mode-locked Lasers," *Opt. Lett.* 16: 1331-1333 (1991).

Project Staff

Professor Hermann A. Haus, Dr. Antonio Mecozzi, Farzana I. Khatri, Yinchieh Lai

Last year we showed that the Gordon-Haus effect that sets a limit on long distance soliton communications could be overcome partially by filtering the pulse stream at every amplifier stage.[6] The carrier frequency of a soliton that deviates from the filter center frequency is pushed by the filter toward the filter center frequency. Since the Gordon-Haus effect is a noise-induced random walk of soliton carrier frequency, filters help to reduce this effect. The filters also help in reducing background noise. Indeed, the net linear bandwidth of the transmission link is greatly reduced by the cascade of the filters so that linear high-bitrate communications are impossible. Fiber nonlinearity allows solitons to recover their spectral width when it has been reduced by filtering; thus high bit-rate soliton pulse trains can be transmitted. The same proposal was made independently by Hasegawa and Kodama at Bell Laboratories.[7] The scheme permits wavelength multiplexing if the filters are the Fabry-Perot type with one multiple transmission peak per channel.

Nakazawa of NTT demonstrated a pulse train transmission that also extended the Gordon-Haus limit, using both filters and modulators.[8] This scheme is not readily adaptable to wavelength multiplexed transmission. However, we have now shown that it eliminates the Gordon-Haus limit entirely.[9] A pulse stream of ones and zeros can propagate indefinitely in a fiber ring with gain to compensate for the loss and with filters and modulators synchronized to the pulse stream. The zeros are maintained because the modulators spread the spectrum of the noise accumulating in the time slots occupied by zeros; then the filters absorb it. A fiber ring that operates on this principle can be used as a high bit-rate all-optical memory. We are now investigating how this memory can be used in conjunction with all-optical switches, delay lines, and frequency shifters for the conversion of Time Division Multiplexing (TDM) to Wavelength Division Multiplexing (WDM) and back again.

1.4 Squeezing

Sponsors

Charles S. Draper Laboratories
Contract DL-H-441629
Fujitsu Laboratories
National Science Foundation
Grant ECS 90-12787
U.S. Navy - Office of Naval Research
Grant N00014-92-J-1302

Project Staff

Professor Hermann A. Haus, Keren Bergman, Luc Boivin, Jeffrey K. Bounds, Christopher R. Doerr, Dr. Franz X. Kärtner, Ilya Lyubomirsky, Dr. Masataka Shirasaki

We are continuing our experiments on squeezing with optical fibers. Comparison of our results with those of the IBM group have shown that the degree of squeezing with pulses of 100 ps duration is critically dependent on the Guided Acoustic Wave Brillouin Scattering (GAWBS) in the fiber. The fiber used in our previous experiments had a "window" of low GAWBS within the frequency range in which we observed squeezing (40-80 kHz). We did not obtain squeezing with a fiber given to us by the IBM group which showed much higher GAWBS in the same frequency regime. This finding prompted us to look for ways to eliminate GAWBS. The IBM group has already proposed and demonstrated squeezing with reduced GAWBS using subpicosecond pulses; the shorter the pulses, the less GAWBS is excited. Another advantage presented by shorter pulses of a given energy is that squeezing can be achieved in short fibers (< 1 m), further reducing GAWBS. C. Doerr has reproduced these results in our laboratory. There are two other ways of reducing GAWBS:

1. A rapid phase modulation of the local oscillator (> 1 GHz) can cancel out the GAWBS upon detection.[10]

---

6 A. Mecozzi, J.D. Moores, H.A. Haus, and Y. Lai, "Soliton Transmission Control," *Opt. Lett.* 16: 1841-1843 (1991).

7 Y. Kodama and A. Hasegawa, "Generation of Asymptotically Stable Optical Solitons and Suppression of the Gordon-Haus Effect," *Opt. Lett.* 17: 31-33 (1992).

8 M. Nakazawa, E. Yamada, H. Kubota, and K. Suzuki, "10 Gbit/s Soliton Transmission over One Million Kilometres," *Electron. Lett.* 27: 1270-1272 (1991).

9 H.A. Haus and A. Mecozzi, "Long-term Storage of a Bit Stream of Solitons," *Opt. Lett.* 17: 1500-1502 (1992).

10 M. Shirasaki and H.A. Haus, "Reduction of Guided-acoustic-wave Brillouin Scattering Noise in a Squeezer," *Opt. Lett.* 17: 1225-1227 (1992).

2. A rapid repetition rate of the pulses (1 GHz) puts the GAWBS spectrum into a frequency regime that does not convolve to low frequencies upon detection.

We have demonstrated successfully scheme 1,[11] which was employed in conjunction with a phase measurement in a Mach-Zehnder interferometer achieving a noise floor 3 dB below the shot noise level. This is the first demonstration of the use of Kerr-squeezed vacuum for an improved phase measurement. We are presently working on scheme 2.

The theory of squeezing requires a self-consistent analysis of nonlinear optical processes. Every quantum measurement employs a nonlinear device. With a self-consistent, yet simple quantum theory of nonlinear devices, one can develop a self-consistent theory of quantum measurement. Taking advantage of this fact, we have analyzed some basic quantum measurements in which we have quantized not only the process to be measured, but also the measurement equipment. Paradoxes of quantum measurement, some of long standing, can be eliminated in this way.[12]

1.5 Integrated Optics Components: The Channel Dropping Filter

Sponsors

National Center for Integrated Photonics
National Science Foundation
Grant ECS 90-12787

Project Staff

Professor Hermann A. Haus, Jay N. Damask, Professor Leslie A. Kolodziejski, Professor Henry I. Smith, Gale S. Petrich, Vincent V. Wong

The Channel-Dropping Filter (CDF), proposed by Haus and Lai,[13] is a novel narrow-band integrated optical filter highly suitable for wavelength-division demultiplexing of optically transmitted bitstreams. The novel architecture of the CDF allows "in-line" filtering of a WDM bitstream.[14] This is in contrast with other currently proposed filters, all of which require the termination of the entire bitstream to resolve the frequency components. Within the past year, we have shown the application of the CDF for phase control of optically controlled phased-array radars and wide area synchronous clock distribution.

The CDF is an integrated optical device that is constructed with three parallel waveguides and quarter-wave shifted distributed-feedback (DFB) gratings. The center guide, the bus, carries the WDM bitstream. On the two side guides, the receiver and mirror, spacially coherent DFB gratings are patterned.

Two prototypes of the CDF are being developed at MIT. One is based on the silica-on-silicon materials system, developed in the Integrated Circuits Laboratory at MIT. While this system is optically passive, its low loss will allow for the strong optical resonances required for proper operation. The other is based on the InGaAsP/InP semiconductor materials system, developed in the Photonic Semiconductors Laboratory in collaboration with Professor L.A. Kolodziejski. This optically active system will allow for optical amplification to overcome the intrinsic material loss as well as allow tuning of the filter frequency. In both cases, x-ray nanolithography is necessary to pattern the 5100 Å and 2300 Å period gratings for the two respective materials systems. The x-ray technology has been developed in the Submicron Structures Laboratory in collaboration with Professor H.I. Smith.

1.6 Tunable Semiconductor Lasers

Sponsor

National Center for Integrated Photonics

Project Staff

Professor Clifton G. Fonstad, Professor Hermann A. Haus, Paul S. Martin

Wavelength Division Multiplexing (WDM) applications such as the channel dropping filter proposed

---

[11] K. Bergman, C.R. Doerr, H.A. Haus, and M. Shirasaki, "Sub-shot Noise Measurement with Fiber Squeezed Optical Pulses," *Opt. Lett.*, forthcoming.

[12] F.X. Kärtner and H.A. Haus, "Quantum Nondemolition Measurements and the 'Collapse of the Wave Function'," *Phys. Rev. A*, forthcoming.

[13] H.A. Haus and Y. Lai, "Quantum Theory of Soliton Squeezing: A Linearized Approach," *J. Opt. Soc. Am. B* 7: 386-392 (1990).

[14] J.N. Damask and H.A. Haus, "Wavelength-division Demultiplexing Using Channel-dropping Filters," *IEEE J. Lightwave Tech.*, forthcoming.

by H.A. Haus and Y. Lai[15] require tunable lasers and/or optical amplifiers. Simulations we performed have shown that the three terminal Independently Addressable Asymmetric Double Quantum Well (IAADQW) structure we proposed has a tuning range of more than 20 nm about a center wavelength of 1.5 μm. This is significantly larger than the continuous tuning range of both three-section Distributed Bragg Reflector (DBR) and Tunable Twin-Guide (TTG) lasers that are competing for use in WDM systems. In addition to wide tuning range, the IAADQW is a three-terminal device so light output power can be kept constant during tuning.

Fabrication of the IAADQW devices has begun using a self-aligned technique we developed. A single photolithography step defines a metal layer which we use as:

1. An etch mask for the definition of an optical waveguide using Reactive Ion Etching (RIE);
2. An ion implant mask that we use to confine the current injection in the lower quantum well;
3. A contact to the upper quantum well.

Use of this technique eliminates critical lithographic alignments that could make the fabrication of three terminal devices prohibitively complex.

1.7 Nonlinear Properties of InGaAsP Optical Amplifiers

Sponsors

Joint Services Electronics Program
Contract DAAL03-92-C-0001
National Center for Integrated Photonics Technology
National Science Foundation
Grant EET 88-15834
U.S. Air Force - Office of Scientific Research
Contract F49620-91-C-0091

Project Staff

Professor Erich P. Ippen, Katherine L. Hall, Ali M. Darwish, Gadi Lenz

The nonlinear properties of semiconductor optical amplifiers are of interest because they 1) influence the modulation response and mode stability of diode lasers, 2) limit speed and produce cross-talk between multiplexed signals in optical amplifiers, and 3) may be useful for the design of nonlinear optical waveguide modulators and switches. We use femtosecond optical pulses, tunable near 1.5 μm, to characterize the optical nonlinearities in the gain and index of InGaAsP diodes and optical amplifiers.

During the past year, we measured for the first time the femtosecond gain dynamics of strained-layer multiple-quantum-well (SLMQW) amplifiers using the novel heterodyne pump-probe technique we had previously developed.[16] The heterodyne technique is essential for studying SLMQW devices because their gain is highly anisotropic. This anisotropy is due to the polarization selection rules and the large energy separation between the light-hole and heavy-hole bands. The pump-probe results show a response consistent with spectral hole burning when the diode is biased in the absorption regime. In the gain regime, carriers are heated by free-carrier absorption, and there is a measurable delay (~ 200 fs) in the thermalization of the hot carrier distribution. Subsequent cooling to the lattice temperature follows with a time constant of ~ 1 ps, which is in good agreement with previous results on bulk and unstrained MQW InGaAsP optical amplifiers.

We have also extended the heterodyne pump-probe technique to measure ultrafast index nonlinearities in bulk and SLMQW amplifiers.[17] For these experiments, we use a high-frequency (ham) radio receiver (instead of a spectrum analyzer) to detect the beat between reference and probe pulses because it has AM and FM reception at the same frequency. This new technique for measuring ultrafast index nonlinearities has many advantages over time division interferometer (TDI) techniques. It

---

[15] H.A. Haus and Y. Lai, "Quantum Theory of Soliton Squeezing: A Linearized Approach," *J. Opt. Soc. Am. B* 7: 386-392 (1990).

[16] K.L. Hall, G. Lenz, and E.P. Ippen, "Novel, Heterodyne Pump-Probe Measurement of Femtosecond Nonlinearities in Waveguides," *Conference on Lasers and Electro-optics Technical Digest,* Anaheim, California, 1992, paper no. JThF4; K.L. Hall, G. Lenz, E.P. Ippen, U. Koren, and G. Raybon, "Carrier Heating and Spectral Hole Burning in Strained-Layer Multiple Quantum Well Lasers at 1.5 μm," *Appl. Phys. Lett.* 61: 2512 (1992).

[17] K.L. Hall, A. Darwish, E.P. Ippen, U. Koren, and G. Raybon, "Femtosecond Index Nonlinearities in InGaAsP Optical Amplifiers," *Appl. Phys. Lett.,* forthcoming; K.L. Hall, A.M. Darwish, E.P. Ippen, U. Koren, and G. Raybon, "Subpicosecond Index Nonlinearities in InGaAsP Diode Laser Amplifiers," *Conference on Lasers and Electro-optics Technical Digest,* Baltimore, Maryland, 1993, paper no. JThA2, forthcoming.

requires no stabilization of the interferometer arms, no balanced detector to eliminate signals due to probe amplitude changes, and it can be used with either copolarized or cross-polarized pump-probe beams. Our results suggest that index nonlinearities are due to an ultrafast optical Kerr effect as well as to carrier heating. The measured n_2 in these diodes ranged from -2×10^{-12} cm^2/W to -6×10^{-12} cm^2/W, depending on the pump-probe polarization orientation and the diode active structure (bulk vs. SLMQW). These are the first pump-probe measurements of index nonlinearites in InGaAsP diodes. Preliminary results for optical switching applications suggest that 150 fs pulses with only 3 pJ of pulse energy can be used to induce large gain (Δ T/T = 95 %) and index ($\Delta\Phi = 0.75\pi$) changes in diodes biased at the transparency point. In this case, the gain and index nonlinearities have recovered completely after 5 ps.

1.8 Ultrafast Index Nonlinearities in Active Waveguides

Sponsors

National Center for Integrated Photonics Technology
National Science Foundation
Grant EET 88-15834
U.S Air Force - Office of Scientific Research
Contract F49620-91-C-0091

Project Staff

Professor Erich P. Ippen, David J. Dougherty, Charles T. Hultgren

Active optical waveguides exhibit large and potentially useful ultrafast nonlinearities. They are attractive structures for use in applications because the carrier density in the active region is easily varied, and thus, the magnitude and recovery time of a given nonlinearity can be controlled. For example, ultrafast index of refraction nonlinearities due to nonequilibrium carriers could become the basis for a controllable all-optical switch. The realization of such a device requires knowledge of how active waveguides respond to optical excitation.

With these ideas in mind, our aim for this project is to use short optical pulses to investigate and characterize the gain and refractive index nonlinearities exhibited by active waveguides. The waveguides we study consist of bulk AlGaAs diode lasers (Hitachi HLP1400) with anti-reflection coatings deposited on the facets. Such a device functions as an active optical waveguide with gain provided by bias current injected into the device. Our previous pump-probe studies employed a dye laser system that produced optical pulses 400 femtoseconds in duration. These measurements revealed that transient carrier heating and the optical Stark effect are the dominant ultrafast refractive index nonlinearities in these devices.

We recently upgraded our source to a modelocked Ti:sapphire laser system that produces pulses as short as 70 femtoseconds. The short pulses and wide tuning range afforded by this new laser system have enabled us to perform detailed studies of above- and below-band gap dynamics in active waveguides.[18] These recent studies have led to further interesting findings about refractive index nonlinearities. In a series of pump-probe measurements conducted with pulses tuned below the active region's band gap energy, we have observed a transient caused by carrier heating with a recovery time of ~1.3 picoseconds. The only method by which carriers can be heated by a below-band photon is through free carrier aborption. Thus, our results indicate that significant carrier heating can result from free carrier absorption. In addition, our below-band studies have also shown that there is a delay of about 0.12 picoseconds in the turn-on of the carrier heating dynamic. This indicates that it takes some finite amount of time for free carriers that have absorbed photons to heat up the sea of carriers sitting at the bottom of the band. We have also observed, in above- and below-band measurements, an instantaneous refractive index transient that we attribute to the optical Stark effect. Our measurements show that this instantaneous nonlinearity experiences a resonant enhancement as the pump wavelength is tuned toward an absorption edge. Finally, studies of above-band gain dynamics have revealed evidence for spectral-hole burning.

Our experiments reveal a great deal about fundamental physical processes and carrier relaxation mechanisms in an optically excited semiconductor. In addition, we are also learning about potentially useful nonlinearities in active waveguides. For instance, transient carrier heating and the optical Stark effect are the source of large, ultrafast

[18] C.T. Hultgren, D.J. Dougherty, and E.P. Ippen, "Above- and Below-band Femtosecond Nonlinearities in Active AlGaAs Waveguides," *Appl. Phys. Lett.* 61: 2767 (1992); C.T. Hultgren, K.L. Hall, G. Lenz, D.J. Dougherty, and E.P. Ippen, "Spectral-hole Burning and Carrier Heating Nonlinearities in Active Waveguides," *Proceedings of the O.S.A. Topical Meeting on Ultrafast Electronics and Optoelectronics,* San Francisco, California, January 1993.

refractive index nonlinearities that may be useful in the development of practical photonic devices.

1.9 Femtosecond Pulse Generation and Amplification in F-center Systems

Sponsors

National Center for Integrated Photonics Technology
National Science Foundation
Grant EET 88-15834
U.S Air Force - Office of Scientific Research
Contract F49620-91-C-0091

Project Staff

Professor Erich P. Ippen, Dr. Jeróme M. Paye, Gadi Lenz, Yuzo Hirayama

Modern lightwave communication systems use carrier wavelengths around 1.55 μm because optical fibers have minimum loss and can be tailored to have negligible dispersion in this spectral region. The characteristics of the semiconductor lasers, detectors, optical amplifiers, and modulators used in these systems depend strongly on material properties as well as device structure. High rates of information transmission will be limited in some cases by the nonlinearities and dynamic behavior of these components. At the same time, novel properties of these 1.5 μm materials and structures may make new device architectures possible. To investigate these limits and new possibilities, we have been developing a unique femtosecond laser system. Comprised of an F-center laser oscillator and high power amplifier, it will provide the broadly tunable source and continuum spectroscopic capability needed for such studies.

The cw femtosecond-pulse oscillator is an NaCl:OH^- laser with a center wavelength of 1.58 μm and a tuning range from 1.5 - 1.65 μm. Pulses with durations of about 100 fs are generated using the Additive Pulse Modelocking (APM) technique that was developed in our lab. With this particular laser, we have also discovered a self-starting mode of APM that exhibits highly stable operation and very low noise. This self-starting under cw pumping is particularly useful because it eliminates the noise associated with a modelocked pump laser. Recently, we took advantage of this characteristic in an experiment involving the generation of squeezed light.[19]

Typical pulse energy at the output of our laser is ~1 nJ. This is sufficient for a variety of pump-probe experiments, but for many experiments, including continuum generation, higher pulse energies are required. This year, we built an optical amplifier for the purpose of reaching these energies. We have observed a gain of 10^4 and 10 μJ output pulses using this system. Our amplifier uses a long NaCl:OH^- crystal as the gain medium. The crystal is pumped by a Q-switched Nd:YAG at a rate of 1 KHz. The amplified pulse passes through the amplifier four times with a total transit time still much shorter than the pump pulse. To match oscillator pulses of the KHz pump repetition rate, we have set up a synchronized electro-optic pulse selection system. With further optimization we expect to achieve as much as 100 μJ per pulse. These energies will allow continuum generation making possible new time resolved spectroscopy experiments. These experiments will yield new information on the basic physics of optical devices.

1.10 Coherent Phonons In Electronic Materials

Sponsors

Joint Services Electronics Program
Contract DAAL03-92-C-0001
U.S Air Force - Office of Scientific Research
Contract F49620-91-C-0091

Project Staff

Professor Erich P. Ippen, Tak K. Cheng

Very large amplitude coherent optical phonons can be induced in semimetals and narrow-gap semiconductors and observed using pulses of light that are short in duration compared to the characteristic periods of lattice vibrations. The excitation mechanism for coherent phonons in these materials is attributed to a rapid displacement of the ion equilibrium coordinate induced by electronic excitation.[20] Our current interest in coherent phonons is two-fold: (1) using time-resolved femtosecond spectroscopy to further our understanding of lattice dynamics in

---

[19] C.R. Doerr, I. Lyubomirsky, G. Lenz, J. Paye, H.A. Haus, and M. Shirasaki, "Optical Squeezing with a Short Fiber," paper presented at QELS '93, Baltimore, Maryland, May 1993.

[20] T.K. Cheng, J. Vidal, H.J. Zeiger, E.P. Ippen, G. Dresselhaus, and M.S. Dresselhaus, "Mechanism for Displacive Excitation of Coherent Phonons," *Appl. Phys. Lett.* 59: 1923 (1991); H.J. Zeiger, J. Vidal, T.K. Cheng, E.P. Ippen, G. Dresselhaus and M.S. Dresselhaus, "Theory for Displacive Excitation of Coherent Phonons," *Phys. Rev. B* 45: 768 (1992).

electronic materials, (2) exploiting the coherent phonon phenomena to modulate the physical characteristics of the material at THz frequencies. We are carrying out this work in collaboration with Professor M. Dresselhaus and her group in the Center for Materials Science and Engineering.

Our most recent experiments involving high excitation densities have shown that a solid, upon optical pulse excitation, can undergo coherent oscillation at frequencies which are shifted significantly (greater than 10 percent) from their low excitation values. Furthermore, we have studied the detailed dynamics of how the coherent phonon evolves from its initial frequency-shifted state back to the equilibrium state. These time-domain measurements provide information inaccessible via other spectroscopic techniques and reveal important non-equilibrium behavior of coherent phonons related to lattice anharmonicity and carrier screening.

A highlight of this past year is that we showed, for the first time, the possibility of coupling coherent phonon dynamics to electron dynamics in the limit of large vibrational amplitudes.[21] For example, we investigated Ti_2O_3, a narrow gap semiconductor which undergoes a semiconductor-semimetal transition as a function of temperature. On the basis of x-ray, Raman, and reflectivity measurements, we deduced that the coherent phonons we excite with femtosecond pulses can modulate the interatomic distances in Ti_2O_3 by as much as two percent. In principle, a three percent modulation is enough to modulate the entire semiconductor-semimetal transition. Experimental work in progress is directed at further developing this notion of modulating the physical characteristics of a solid at THz frequencies via optically induced coherent phonons.

1.11 Femtosecond Studies of Fullerenes

Sponsors

Joint Services Electronics Program
Contract DAAL03-92-C-0001
U.S Air Force - Office of Scientific Research
Contract F49620-91-C-0091

Project Staff

Professor Erich P. Ippen, Siegfried B. Fleischer

The soccerball-shaped molecule C_{60} with its high symmetry has generated considerable theoretical as well as experimental research. Some of this interest has been inspired by the discovery of superconductivity with a high transition temperature of 18 K and 28 K for this third form of carbon if doped with potassium and rubidium, respectively.

The high symmetry (I_h) of C_{60} imposes strong selection rules on phonon mediated excited states transitions. It is therefore interesting to study the processes of electronic and vibrational energy decay in the excited singlet and triplet states in C_{60} versus those for the C_{60}^{3-} ions in doped samples which are metallic and of lower symmetry. A fundamental question is whether the fullerenes with their unusual structure present excited state features that are distinct from other aromatic molecules. Optical pump-probe experiments allow us to monitor the dynamics of the scattering between excited states and thus give information about the electronic structure as well as the strength of the coupling to phonons. We are performing such studies in collaboration with Professor M. Dresselhaus and with Professor P. Ecklund of the University of Kentucky.

The undoped (C_{60}) and doped (K_3C_{60}, Rb_3C_{60}) films used for our pump-probe measurements were thin homogeneous polycrystalline films deposited on quartz substrates with a typical film thickness of 2000 Å. To prevent oxygen contamination all the samples were sealed off in helium. Femtosecond dynamics were induced and observed, in reflectivity and transmission at λ=625 nm, using pulses from a colliding-pulse modelocked (CPM) dye laser. Both the K and Rb doped films show approximately the same fast decay on the order of 0.2 ps. This is much faster than the monitored response of C_{60}, which exhibits a decay rate on the order of 30 ps, with a fast initial component on the order of 1 ps.[22]

The difference in these decay rates reflects the molecular character of C_{60} and the band-like character of M_3C_{60} (M=K, Rb). We attribute the measured nonexponential decay of the C_{60} films to the relaxation of excited state carriers from their initial singlet states to lower lying excited triplet states. This is a relatively slow process because the scattering is only on-ball via coupling to vibrational

---

[21] T.K. Cheng, L. Acioli, E.P. Ippen, J. Vidal, H.J. Zeiger, G. Dresselhaus, and M.S. Dresselhaus, "Modulation of a Semiconductor-to-Semimetal Transition at Seven Teraherz via Coherent Lattice Vibrations," *Appl. Phys. Lett.*, forthcoming.

[22] S.B. Fleisher, E.P. Ippen, G. Dresselhaus, M.S. Dresselhaus, A.M. Rao, P. Zhou, and P.C. Ecklund, "Femtosecond Optical Dynamics of M_3C_{60}," *Appl. Phys. Lett.*, forthcoming

modes. For the doped samples the half filled LUMO-derived conduction band gives rise to parity allowed pump-induced transitions of electrons to even higher lying bands. K_3C_{60} and Rb_3C_{60} are metallic and therefore exhibit properties related to narrow bands rather than vibrationally broadened molecular states (as in the case of C_{60}). Subsequent to their optical excitation, the carriers created in both the initial and final states undergo thermal equilibration within each band via Coulomb scattering and also on a slower or competing time scale via electron-phonon coupling. Both processes also scatter excited-state electrons out of their initial states into states with different symmetry and thus modulates the absorption cross section. For a more detailed understanding of the electronic structure and the scattering mechanisms in these materials, wavelength selective pump-probe investigations will be performed.

1.12 Ultrashort Pulse Generation in Solid State Lasers

Sponsors

Joint Services Electronics Program
Contract DAAL03-91-C-0001
National Science Foundation
Fellowship ECS-85-52701
U.S. Air Force - Office of Scientific Research
Contract F49620-91-C-0091
U.S. Navy - Office of Naval Research (MGH)
Contract N00014-91-C-0084

Project Staff

David Huang, Joseph M. Jacobson, Malini Ramaswamy, Morrison Ulman, Dr. Lucio H. Acioli, Dr. Joseph A. Izatt, Professor James G. Fujimoto

1.12.1 Fundamental Limits to Ultrashort Pulse Generation

The development of techniques for the generation of ultrashort laser pulses is essential for studies of ultrafast pheonomena as well as high speed optical communications and signal processing applications. The problem of exploring the limits of short pulse modelocked laser performance is an important issue in femtosecond optics. The time resolution of ultrafast measurements is limited only by the shortest laser pulse durations than can be generated. In addition, the bandwidths available from short pulses make possible the use of spectral shaping and synthesis techniques.

Recent advances have made it possible to generate pulse durations of less than 100 fs using third generation solid state laser technology. Solid state lasers feature high energy storage and high power operation and can be engineered into a compact and relatively low cost short pulse technology. The next milestone in ultrafast phenomena will be the development of solid state laser systems which can reliably generate pulse durations of a few femtoseconds. Advancing the performance of solid state laser technology will require fundamental studies of pulse generation and pulse shaping mechanisms as well as the development of new pulse generation techniques. During the past year our research has focussed on exploring the fundamental limits for short pulse generation in solid state lasers and developing techniques which have the potential for generating pulse durations of less than 10 fs.

The fundamental issue that underlies the development of sub 10 fs lasers is how can one acheive the minimum possible pulsewidth and utilize the full bandwidth that is available from a given laser gain media. $Ti:Al_2O_3$ is an especially attractive material for the study of femtosecond pulse generation because of its large gain bandwidth. The tuning range of $Ti:Al_2O_3$ is from 670 nm to greater than 1000 nm. From the energy time uncertainty relationship, the pulsewidth scales inversely with the bandwidth of the medium. More specifically, the analytic theory of Additive Pulse Modelocking (APM) as developed by Haus et al.[23] predicts that the shortest pulse scales inversely with the gain bandwidth multiplied by the square root of the saturable absorption. Assuming a saturable absorber loss modulation of 1 percent, the bandwidth of $Ti:Al_2O_3$ should support pulses of 10 fs. In addition, the use of intracavity self-phase-modulation and negative group velocity dispersion can further reduce the pulse width by a factor of three.[23] Thus, in theory, pulses of 3 fs should be acheivable directly from a $Ti:Al_2O_3$ laser.

---

[23] H.A. Haus, J.G. Fujimoto, and E.P. Ippen, "Structures for Additive Pulse Modelocking," *J. Opt. Soc. Am. B* 8: 2068-2076 (1991).

1.12.2 Short Pulse Generation using Intracavity Dispersion Compensation

One central issue in the generation of extremely short pulse durations is the control of very broad bandwidth optical signals. The spectral width of a laser pulse is inversely proportional to its duration; in the 10 fs regime for a pulse in the near infrared, the pulse bandwidth will be more than 60 nm or almost ten percent of the carrier frequency. One approach for optimizing laser performance is to compensate intracavity dispersion. Previous results in pulse compression studies[24] and in laser modelocking[25] have shown that control of higher order dispersion is essential in short pulse generation. Second order, or group velocity, dispersion may be compensated with a pair of either prisms or gratings. The low loss of prisms inserted at Brewster's angle has allowed their use inside laser cavities; they are essential components of both colliding pulse modelocked dye lasers and Kerr lens mode locked solid state lasers. While the dominant effect of both prism and grating pairs is to correct second order dispersion, they simultaneously introduce third order effects. Luckily, the sign of the third order contribution of gratings is opposite to that of prisms. A combination of gratings and prisms was used in an extracavity pulse compression experiment to produce 6 fs pulses, the current world record.[24]

Working in collaboration with CVI Inc., we have designed and built a thin film optical element that introduces only third order dispersion and has low loss necessary for intracavity use. Our device, a Gires-Tournois interferometer (GTI), is fabricated on a high reflecting mirror substrate and permits the independent control second and third order intracavity dispersion. The amount of third order dispersion may be selected by varying the number of bounces of the laser beam off the GTI. This technique has allowed us to reduce the pulse duration in a Kerr lens modelocked Ti:Al_2O_3 laser from 45 fs to 28 fs. We have performed detailed studies which characterize the intracavity dispersion in the Ti:Al_2O_3 laser in order to demonstrate the role of third order dispersion compensation for the optimization of femtosecond laser performance.[26]

Approaches for optimizing pulse duration performance have emerged as an active area of research in recent months. Since our demonstration of the GTI as a third order dispersion compensating device, a number of other approaches for controlling dispersion have also been investigated by us as well as other research groups. These techniques include the use of specialized glasses for prisms and multiple prism schemes. The current record for pulsewidth using this approach is 11 fs.[27] Further improvements in the pulse duration generated directly from a laser will probably require other pulse compression and shaping techniques as well as laser intracavity dispersion compensation.

In addition to optimizing laser performance, we are also investigating alternative strategies for generating short pulses. Our studies focus on exploiting the short pulse durations and high peak intensity of the pulses for external pulse compression. We are pursuing two approaches to achieve this compression and study its limits. We have recently built a Kerr lens modelocked Ti:Al_2O_3 laser which uses minimized third order dispersion to generate pulse durations of less than 30 fs. The high peak energies and short pulsewidths of these pulses suggest that good compression factors may be achieved using using optical fiber pulse compression techniques to attain durations of 10 fs or less with pulse energies of 1 to 2 nJ at repetion rates of 100 Mhz. Investigation of these pulse compression techniques and factors which govern their performance are currently underway.

1.12.3 Cavity Dumped Femtosecond Laser Sources

Another complementary approach for short pulse generation is the development and investigation of techniques for cavity dumping modelocked femtosecond solid state lasers. These studies are important because they provide increased pulse energies without using amplification. These

---

[24] R.L. Fork, C.H. Brito-Cruz, P.C. Becker, and C.V. Shank, "Compression of Optical Pulses to Six Femtoseconds by Using Cubic Phase Compensation," *Opt. Lett.* 12: 483 (1987).

[25] R.L. Fork, C.H. Brito Cruz, P.C. Becker, and C.V. Shank, "Third-order Group Velocity Dispersion in a Colliding-pulse Mode-locked Dye Laser," *Opt. Lett.* 15: 1374-1376 (1990).

[26] J.M. Jacobson, K. Naganuma, H.A. Haus, J.G. Fujimoto, and A.G. Jacobson, "Femtosecond Pulse Generation in a Ti:Al_2O_3 Laser by Using Second- and Third-order Intracavity Dispersion," *Opt. Lett.* 17: 1608 (1992).

[27] M.T. Asaki, C.-P. Huang, D. Garvey, J. Zhou, H.C. Kapteyn, and M. Murnane, "Generation of 11 fs Pulses from a Self Mode-locked Ti:Sapphire Laser," *Opt. Lett.*, forthcoming.

increased pulse energies from this laser will make it ideal for pulse compression as well as for femtosecond studies of nonlinear processes.

In preliminary studies using the Kerr lens modelocked Ti:Al_2O_3 laser we have demonstrated cavity dumping using an intracavity acousto-optic Bragg cell. Pulse durations as short as 50 fs with 100 nJ pulse energies were generated at a 900 KHz repetition rate. In addition to the generation of high energy short pulses, cavity dumping provides an approach for studying the pulse formation dynamics in the laser. One of the surprising findings of our preliminary studies was that relatively high dumping rates can be achieved without significant disruption of the modelocking and pulse formation process.

Further studies are currently underway to extend these techniques to yield pulse durations of less than 30 fs with higher pulse energies. The development of a cavity dumped Kerr lens modelocked Ti:Al_2O_3 laser is significant because it represents a simpler and lower cost alternative approach to amplification for achieving increased pulse energies.

1.13 Studies of Ultrafast Phenomena in Materials

Sponsors

Joint Services Electronics Program
Contract DAAL03-91-C-0001
National Science Foundation
Fellowship ECS-85-52701
U.S. Air Force Office of Scientific Research
Contract F49620-91-C-0091
U.S. Navy - Office of Naval Research
Grant N00014-91-J-1956

Project Staff

Malini Ramaswamy, Chi-Kuang Sun, Dr. Lucio H. Acioli, Dr. Fabrice Vallee, Professor Erich P. Ippen, Professor James G. Fujimoto

1.13.1 Femtosecond Carrier Dynamics in AlGaAs

The design and optimization of high speed electronic and optoelectronic devices depends on knowledge of the dynamics of transient electron and hole populations in semiconductor materials. Carrier dynamics determine the fundamental limits of device speed. For example, intervalley electron scattering is largely responsible for the high field transport properties of GaAs and AlGaAs. For ideal device design it should be possible to predict the time and energy evolution of a excited carrier distribution in the bandstructure of a semiconductor. Electron-electron scattering times are as short as several femtoseconds. Therefore, an accurate model of carrier behavior must have the ability to predict transient effects on the femtosecond time scale.

Working in collaboration with solid state theoretical physicists at the University of Florida, we have developed a collaborative research program which combines state of the art experimental and theoretical techniques to perform detailed investigations of carrier dynamics in GaAs and AlGaAs on a femtosecond scale. Using femtosecond laser experimental studies at MIT and ensemble Monte Carlo computer simulations at the University of Florida, we have been able to experimentally measure and theoretically model the various scattering processes and relaxation mechanisms of excited carrier distributions. The result of our work is a model that may be extended to predict transient carrier dynamics in a variety of different excitation conditions in semiconductors.

Last year, we performed a series of experimental studies on AlGaAs using a tunable femtosecond laser system.[28] By systematic variation of the wavelength and spectrum of the femtosecond laser pulses, the evolution of optically excited carrier distributions initially generated in different regions of the band can be systematically investigated. The laser system used for these investigations is an amplified colliding pulse modelocked (CPM) laser. Optical pulses as short as 35 femtoseconds from the CPM are amplified to microjoule energies in a two stage dye amplifier pumped by a copper vapor laser. The amplified pulses are then focused on a flowing jet of ethylene glycol to produce a femtosecond white light continuum. A Fourier frequency filter is used to select the desired spectrum

[28] M. Ulman, D.W. Bailey, L.H. Acioli, F.G. Vallee, C.J. Stanton, E.P. Ippen, and J.G. Fujimoto, "Femtosecond Tunable Nonlinear Absorption Saturation Spectroscopy in $Al_{0.1}Ga_{0.9}As$," *Phys. Rev. B*, forthcoming.

from the continuum.[29] Fourier synthesized pulses may be generated with arbitrary spectral or temporal profiles; in our experiment we are primarily concerned with wavelength and bandwidth since they determine the initial state of carriers excited to the conduction band.

Using this laser source, pump probe studies were performed on AlGaAs samples. The mole fraction of Al in the AlGaAs sample was chosen to vary the bandstructure and isolate specific optical transitions. The result of the experimental part of our investigation is a comprehensive set of pump probe differential transmission traces. The data span a range of wavelengths and excited carrier densities, and are recorded for the first thousand femtoseconds after initial excitation.

In another study we investigated excited carrier dynamics in the presence of a cold carrier plasma.[30] This situation is analogous to the conditions found in a diode laser. We developed a novel three pulse pump probe technique to investigate the transient carrier dynamics after the generation of carriers with a pre-pulse. The first pulse excites carriers which relax to a quasiequilibrium, cold distribution before the pump probe measurement takes place. In this experiment we varied the bandstructure of the sample instead of tuning the femtosecond laser. With this technique we investigated effects above and below the cold plasma Fermi level and the role of intervalley scattering. The presence of the cold plasma induces only a small increase in the hot carrier thermalization rate even for high cold plasma densities. In fact, the thermalization of a low density, hot carrier distribution interacting with a cold, high density photoexcited plasma occurs on a time scale longer than intervalley scattering in GaAs.

While the femtosecond pump probe technique provides the highest temporal resolution available today, the interpretation of the experimental results is often complex. We use state of the art computer simulations for two purposes: 1) to keep track of the large number of optical transitions and scattering channels in semiconductor experiments, and 2) to deduce fundamental physical information, such as the time dependent carrier distributions, from differential transmission data. Simple analytical models provide physical insight, but do not yield detailed correspondence with experimental results. Our theoretical model begins with a 30 band, full zone **k** • **p** calculation of the semiconductor bandstructure. Anisotropy and hole warping effects are included. An ensemble Monte Carlo simulation of 40,000 electrons and holes tracks the time development of the distribution functions.[31] The final step is a calculation of the differential transmission which is then compared directly with the experimental traces. Fundamental parameters such as the deformation potential constant and carrier scattering rates are then deduced. A further advantage of the simulation technique is that the strengths of different scattering channels may be artificially varied and the sensitivity of the data to specific processes may be assessed.

1.13.2 Nonequilibrium Electronic Effects in Metals

Studies of interactions of free carriers between themselves and their environment constitute one of the major problems of solid state physics. This has been addressed directly in the time domain employing femtosecond techniques both in semiconductors and metals. Metals are especially interesting because they have a very high electron density and their behavior can be modeled relatively simply. The possibility of creating and probing a transient nonequilibrium electron population in metal with ultrashort laser pulses has been demonstrated by different groups.[32] In previous experiments, electron-electron interactions were assumed to be sufficiently fast to thermalize the

---

29 A.M. Weiner, J.P. Heritage, and E.M. Kirschner, "High Resolution Femtosecond Pulse Synthesis," *J. Opt. Soc. Am. B* 5: 1563 (1988).

30 L.H. Acioli, M. Ulman, F. Vallee, and J.G. Fujimoto, "Femtosecond Carrier Dynamics in the Presence of a Cold Plasma in GaAs and AlGaAs," submitted to *Appl. Phys. Lett.*

31 D.W. Bailey, C.J. Stanton, and K. Hess, "Numerical Studies of Femtosecond Carrier Dynamics in GaAs," *Phys. Rev. B* 42: 3423 (1990).

32 G.L. Eesley, "Observation of Nonequilibrium Electron Heating in Copper," *Phys. Rev. Lett.* 51: 2140 (1983); H.E. Elsayed-Ali, T.B. Norris, M.A. Pessot and G.A. Mourou, "Time-resolved Observation of Electron-phonon Relaxation in Copper," *Phys. Rev. Lett.* 58: 1212 (1987); R.W. Schoenlein, W.Z. Lin, J.G. Fujimoto and G.L. Eesley, "Femtosecond Studies of Nonequilibrium Electronic Process in Metals," *Phys. Rev. Lett.* 58: 1680 (1987); R.H.M. Groeneveld, R. Sprik and A. Lagendijk, "Ultrafast Relaxation of Electrons Probed by Surface Plasmons at a Thin Silver Film," *Phys. Rev. Lett.* 64: 784 (1990); S.D. Brorson, A. Kazeroonian, J.S. Moodera, D.W. Face, T.K. Cheng, E.P. Ippen, M.S. Dresselhaus, and G. Dresselhaus, "Femtosecond Room-temperature Measurement of the Electron-phonon Coupling Constant λ in Metallic Superconductors," *Phys. Rev. Lett.* 64: 2172 (1990); S.D. Brorson, J.G. Fujimoto, and E.P. Ippen, "Femtosecond Electronic Heat-transport Dynamics in Thin Gold Film," *Phys. Rev. Lett.* 59: 1962 (1987); H.E.

electron gas on a time scale of the order or shorter than the laser pulse duration, although some deviations from an instantaneous response were observed.[33] Recent investigations using transient photoemission have demonstrated the existence of non-Fermi electron distributions with thermalization times as long as 600 fs. These results were observed in gold film for large changes of the electron temperature (of the order of 400°K) with a limited time resolution.[34] Similar conclusions were drawn at lower laser fluence by analyzing the temperature dependence of the optically measured electron-phonon interaction time in gold and silver.[35]

In order to analyze the effect of the non-instantaneous electron-electron interaction on the optical response of a metal film, recently we have performed transient reflectivity and transmissivity measurements of electron temperature dynamics.[36] Studies were performed in the perturbative regime where the measured changes in reflectivity and transmissivity can be directly connected to the electron distribution. In contrast to previous experiments, we use a multiple wavelength femtosecond pump-probe technique to excite the electron gas with a infrared pulse (from a mode-locked Ti:Al_2O_3 laser with 120 fs pulsewidth and 880-1065 nm wavelength) and probe changes in optical properties using frequency doubled wavelength in the visible (440-532.5 nm). This technique permits a more definitive measurement of electron dynamics by seperating the effects of pump induced transitions from those monitored by the probe. Experiments were performed on thin gold films because the band structure of gold is relatively well known and band to band transition can be easily probed by a frequency doubled Ti:Al_2O_3 femtosecond laser.

Measurements show evidence for non-Fermi electron distributions with a electron thermalization time of ~500 fs and an electron-lattice cooling time of 1 ps, independent of the laser fluence in the range of 2.5 mJ/cm² - 200 mJ/cm² (corresponding to estimated peak temperature change 3-200°K).[36] A simple model based on carrier population changes and curved *d*-band was developed to describe the behavior of the system. The diffusion in the optically thin sample is neglected and the electron distribution change is simply seperated to two parts: Fermi and non-Fermi, coupled by an electron gas thermalization term. Excellent qualitative correspondence between theory and experiment was obtained.

Our measured electron thermalization time is comparable to the previous estimations.[37] On the basis of the very high electron density of metals, one would expect very fast electron-electron interactions. However, the interaction efficiency is considerably reduced by phase space filling which blocks most of the energetically possible interaction channels and by screening which considerably reduces the efficiency of the Coulombic interaction. Our results are significant because they provide some of the first detailed information on non-Fermi electron dynamics in metals and demonstrate new experimental techniques for their investigation.

1.14 Time Domain Diagnostics of Waveguide Devices

Sponsors

Joint Services Electronics Program
Contract DAAL03-91-C-0001
National Science Foundation
Fellowship ECS-85-52701

Elsayed-Ali, T. Juhasz, G.O. Smith and W.E. Bron, "Femtosecond Thermoreflectivity and Thermotransmissivity of Polycrystalline and Single-crystalline Gold Film," *Phys. Rev. B* 43: 4488 (1991).

[33] R.W. Schoenlein, W.Z. Lin, J.G. Fujimoto and G.L. Eesley, "Femtosecond Studies of Nonequilibrium Electronic Process in Metals," *Phys. Rev. Lett.* 58: 1680 (1987); S.D. Brorson, A. Kazeroonian, J.S. Moodera, D.W. Face, T.K. Cheng, E.P. Ippen, M.S. Dresselhaus, and G. Dresselhaus, "Femtosecond Room-temperature Measurement of the Electron-phonon Coupling Constant λ in Metallic Superconductors," *Phys. Rev. Lett.* 64: 2172 (1990).

[34] W.S. Fann, R. Storz, H.W.K. Tom, and J. Bokor, "Direct Measurement of Nonequilibrium Electron-energy Distributions in Subpicosecond Laser-heated Gold Films," *Phys. Rev. Lett.* 68: 2834 (1992).

[35] R.H.M. Groeneveld, R. Sprik and A. Lagendijk, "Effect of a Nonthermal Electron Distribution on the Electron-phonon Energy Relaxation Process in Noble Metals," *Phys. Rev. B* 45: 5079 (1992).

[36] C.-K. Sun, F. Valleeé, L. Acioli, E.P. Ippen, J.G. Fujimoto, "Femtosecond Investigation of Electron Thermalization in Gold," submitted to *Appl. Phys. Lett.*

[37] W.S. Fann, R. Storz, H.W.K. Tom, and J. Bokor, "Direct Measurement of Nonequilibrium Electron-energy Distributions in Subpicosecond Laser-heated Gold Films," *Phys. Rev. Lett.* 68: 2834 (1992); R.H.M. Groeneveld, R. Sprik and A. Lagendijk, "Effect of a Nonthermal Electron Distribution on the Electron-phonon Energy Relaxation Process in Noble Metals," *Phys. Rev. B* 45: 5079 (1992).

U.S. Air Force Office of Scientific Research
Contract F49620-91-C-0091
U.S. Navy - Office of Naval Research
Grant N00014-91-J-1956

Project Staff

Chi-Kuang Sun, Professor James G. Fujimoto

1.14.1 Studies of Gain Dynamics in Strained Layer Diodes

Nonlinear gain and transient carrier dynamics in diode lasers are important because they influence laser linewidth, modulation bandwidth, amplication, and short pulse generation. Previous investigators have performed picosecond and femtosecond pump probe measurements of nonlinear gain dynamics in bulk GaAs,[38] InGaAsP MQW,[39] and InGaAs/InGaAsP strained-layer MQW amplifiers.[40] These studies have shown that nonequilibrium carrier temperature effects play an important role in carrier dynamics. Carrier temperature changes are caused by a number of processes including state filling produced by stimulated transitions, free carrier absorption, and two photon absorption. Previous studies[40] have shown that free carrier absorption play a dominant role in carrier heating. A ~ 150 fs relaxation time had been observed which was attributed to either spectral hole burning or turn on delay of free carrier heating. In addition to nonlinear gain, carrier dynamics also produce nonlinear index effects such as self phase modulation.[41]

Recently we invented a new technique for performing independent multiple wavelength pump-probe measurement in waveguide devices.[42] The output of a Kerr lens mode-locked Ti:Al_2O_3 laser was coupled to an optical fiber to produce a self phase modulation broadened spectral bandwidth ~ 50 nm FWHM. After the fiber, the beam was split into a pump and a probe, which were directed into two spectral windowing assemblies[43] to produce synchronous independent different-frequency pulses. This approach represents a powerful method for performing experimental studies since the pump and probe wavelengths can be varied independently and thus energy relaxation dynamics can be explicitly measured.

Working in collaboration with investigators at MIT Lincoln Laboratory, we have performed the first studies of carrier dynamics in InGaAs/GaAs strained layer quantum well diode lasers. Strained layer quantum well devices represent one of the most active and technologically promising areas of current optoelectronics device research. Strained layer materials provide an added degree of freedom by allowing the epitaxial growth of nonlattice-matched materials. High power, high efficiency, long lifetime, and low threshold current density[44] semiconductor lasers have been achieved in InGaAs strained layer devices.

Our studies were performed using a broad-area InGaAs/AlGaAs graded-index separate-confinement heterostructure single quantum well (GRIN-SCH

---

38 M.S. Stix, M.P. Kesler, and E.P. Ippen, "Observations of Subpicosecond Dynamics in GaAlAS Laser Diodes," *Appl. Phys. Lett.* 48: 1722-1724 (1986); M.P. Kesler and E.P. Ippen, "Subpicosecond Gain Dynamics in GaAlAs Laser Diodes," *Appl. Phys. Lett.* 51: 1765-1767 (1987).

39 K.L. Hall, J. Mark, E.P. Ippen, and G. Eisenstein, "Femtosecond Gain Dynamics in InGaAsP Optical Amplifiers," *Appl. Phys. Lett.* 56: 1740-1742 (1990); Y. Lai, K.L. Hall, E.P. Ippen, G. Eisenstein, "Short Pulse Gain Saturation in InGaAsP Diode Laser Amplifiers," *IEEE Photonics Tech. Lett.* 2: 711-713 (1990); K.L. Hall, Y. Lai, E.P. Ippen, G. Eisenstein, and U. Koren, "Femtosecond Gain Dynamics and Saturation Behavior in InGaAsP Multiple Quantum Well Optical Amplifiers," *Appl. Phys. Lett.* 57: 2888-2890 (1990).

40 K.L. Hall, G. Lenz, E.P. Ippen, U. Koren, and G. Raybon, "Carrier Heating and Spectral Hole Burning in Strained-Layer Quantum Well Laser Amplifiers at 1.5 μm," submitted to *Appl. Phys. Lett.*

41 N.A. Olsson and G.P. Agrawal, "Spectral Shift and Distortion Due to Self-phase Modulation of Picosecond Pulses in 1.5 μm Optical Amplifiers," *Appl. Phys. Lett.* 55: 13 (1989); R.S. Grant and W. Sibbett, "Observations of Ultrafast Nonlinear Refraction in an InGaAsP Optical Amplifier," *Appl. Phys. Lett.* 58: 1119 (1989); P.J. Delfyett, Y. Silberberg, and G.A. Alphonse, "Hot-carrier Thermalization Induced Self-phase Modulation in Semiconductor Travelling Wave Amplifiers," *Appl. Phys. Lett.* 59: 10 (1990).

42 C.K. Sun, H.K. Choi, C.A. Wang, and J.G. Fujimoto, "Studies of Carrier Heating in InGaAs/AlGaAs Strained-Layer Quantum-Well Diode Lasers Using a Multiple Wavelength Pump-Probe Technique," *Appl. Phys. Lett.*, forthcoming.

43 A.M. Weiner, J.P. Heritage, and E.M. Kirschner, "High Resolution Femtosecond Pulse Synthesis," *J. Opt. Soc. Am. B* 5: 1563 (1988).

44 H.K. Choi, and C.A. Wang, "InGaAs/AlGaAs Strained Single Quantum Well Diode Lasers with Extremely Low Threshold Current Density and High Efficiency," *Appl. Phys. Lett.* 57: 321 (1990); R.L. Williams, M. Dion, F. Chatenoud, and K. Dzurko, "Extremely Low Threshold Current Strained InGaAs/AlGaAs Lasers by Molecular Beam Epitaxy," *Appl. Phys. Lett.* 58: 1816 (1991).

SQW) ridge waveguide diode laser[45] with a bandgap near 950 nm. Carrier heating was studied by tuning the pump pulse above and below the bandgap while keeping all the other conditions (including the probe) constant. The high sensitivity of the system allowed us to perform the experiment in the low perturbation regime. Different heating and cooling times were measured which reflect different thermalization mechanisms for above and below band pumping. This result shows that free carrier absorption is not always the dominant carrier heating process and stimulated transition induced heating plays an important role in the carrier heating process, at least in strained InGaAs/AlGaAs systems.[46] These studies represent the first pump-probe measurement in InGaAs/AlGaAs strained layer systems. This is also the first multiple wavelength time-domain diagnostics in waveguide structures.

Femtosecond gain dynamics was also investigated using multiple wavelength techniques.[47] Instead of shifting the pump pulse, the bias current was varied so that gain, transparency, and absorption was produced at the pump wavelength. The probe wavelength was in the gain region for all the cases. Carrier temperature changes mediated by both free-carrier absorption and stimulated transitions were observed. Stimulated transition induced carrier cooling was observed in the absorption region. This was the first observation of carrier cooling in GaAs based devices. An increased understanding of the physical mechanisms of gain dynamics from carrier temperature changes is important for the design of new devices. In particular, the reduction of carrier heating has important implications for reducing parasitic gain saturation effects in short pulse modelocked laser diodes and amplifiers.

1.15 Laser Medicine

Sponsors

National Institutes of Health
Grant NIH-5-R01-GM35459-08
U.S. Navy - Office of Naval Research (MGH)
Contract N00014-91-C-0084

Project Staff

Michael R. Hee, David Huang, Dr. Joseph A. Izatt, Dr. Charles P. Lin, Professor James G. Fujimoto

1.15.1 The Ultrashort Pulse Scalpel

The objective of our program is to continue development of an optimized ultrashort pulse laser scalpel for precise intraocular microsurgery. Over the last ten years, short optical pulses have been successfully applied for non-invasive cutting of intraocular structures, for example in posterior capsulotomy and iridotomy. Through the mechanism of laser induced breakdown, photodisruption or cutting of intraocular structures is made possible without the need for intervening surgical incision. To date, the majority of clinical applications of laser induced optical breakdown have utilized nanosecond pulses in the millijoule energy range and single pulse exposures.[48] However, mechanical side effects of laser induced breakdown with nanosecond sources pose potential hazards to adjacent ocular structures and tissues. Our investigations have demonstrated that significant reduction of collateral tissue damage may be achieved through the use of ultrashort pulses. These studies are part of an ongoing collaboration between investigators at MIT, the New England Eye Center of New England Medical Center Hospitals, and the Wellman Laboratories of Photomedicine at Massachusetts General Hospital.

The physical processes which occur in laser induced breakdown include plasma formation, acoustic wave generation, and cavitation. We have

---

[45] C.K. Sun, H.K. Choi, C.A. Wang, and J.G. Fujimoto, "Studies of Carrier Heating in InGaAs/AlGaAs Strained-Layer Quantum-Well Diode Lasers Using a Multiple Wavelength Pump-Probe Technique," *Appl. Phys. Lett.*, forthcoming; C.K. Sun, H.K. Choi, C.A. Wang, and J.G. Fujimoto, "Femtosecond Gain Dynamics in InGaAs/AlGaAs Strained-Layer Quantum-Well Diode Lasers," submitted to *Appl. Phys. Lett.*

[46] C.K. Sun, H.K. Choi, C.A. Wang, and J.G. Fujimoto, "Studies of Carrier Heating in InGaAs/AlGaAs Strained-Layer Quantum-Well Diode Lasers Using a Multiple Wavelength Pump-Probe Technique," *Appl. Phys. Lett.*, forthcoming.

[47] C.K. Sun, H.K. Choi, C.A. Wang, and J.G. Fujimoto, "Femtosecond Gain Dynamics in InGaAs/AlGaAs Strained-Layer Quantum-Well Diode Lasers," submitted to *Appl. Phys. Lett.*

[48] F. Fankhauser, P. Roussel, J. Steffen, E. Van der Zypen, and A. Cherenkova, "Clinical Studies on the Efficiency of High Power Laser Radiation Upon Some Structures of the Anterior Segment of the Eye," *Int. Ophthalmol.* 3: 129 (1981).

studied and compared the mechanisms, scaling behavior, and tissue effects of single pulses in the nanosecond and picosecond ranges.[49] In general, nanosecond and picosecond optical breakdown results in comparable damage zones if the same amount of energy is deposited; however, the threshold energy for breakdown is much lower for picosecond pulses, and near- threshold picosecond pulses produce greatly reduced collateral damage zones. For example, we have demonstrated collateral damage ranges in a corneal endothelial cell model of only 100 microns with 40 picosecond duration pulses at 8 microjoules pulse energy. We have also studied tissue effects (corneal incisions) into the femtosecond domain.[50] Ultrashort pulses with high peak intensities can produce plasma-mediated ablation of transparent tissues, such as the cornea. Picosecond and femtosecond pulse durations have been demonstrated to produce much smoother excision edges and less damage to the adjacent tissue than nanosecond pulses.

Following these initial studies, we have developed a clinically viable picosecond laser scalpel based on a modelocked, Q-switched Nd:YAG laser with external pulse selection. This laser delivers single 100 picosecond duration pulses at a repetition rate variable from 3 to 1000 Hz; each pulse produces minimal collateral damage, while multiple pulses produce a cumulative incision effect. With this laser, we achieve optical breakdown in the deep vitreous with less than 70 microjoules pulse energy, compared to millijoules used in current clinical Q-switched systems. We have performed *in vitro* and *in vivo* studies of vitreous membrane surgery with the high repetition rate picosecond laser. Membrane surgery of the deep vitreous is a very challenging procedure because of the proximity of the retina and the sensitivity of the retina to thermal and/or mechanical injury. Using an *in vitro* vitreous membrane model, we have demonstrated that repetitive picosecond pulses can produce a fine linear incision with ~ 100 micron cut width. Mechanical disruption posterior to the laser focus is also confined to less than 200 microns. We have also performed picosecond laser microsurgery *in vivo* in experimental vitreous membranes in rabbit eyes. Cuts were successfully made through membranes at distances varying from < 100 microns to 3 mm from the retina without causing vitreous hemorrhage and with only minor cell disruption visible upon histological examination. Based in part on these results, the FDA has approved an initial clinical trial of picosecond laser vitreous membrane surgery in human patients. We have also extended the use of picosecond lasers to glaucoma surgical procedures such as iridectomy and ab externo sclerostomy.

In addition to further clinical studies using our current picosecond laser system, we are also developing new laser technology designed specifically for optimizing highly localized photodisruption in transparent structures using laser induced breakdown. These studies are being performed using a flashlamp-pumped titanium-sapphire laser tunable from 700-1000 nm at 20 Hz repetition rate. Flashlamp pumped solid state lasers feature higher pulse energy and lower cost compared to cw laser pumped lasers. Using a combination of active modelocking and passive optical limiting for suppression of relaxation oscillations, we have obtained modelocked pulses of approximately 100 picoseconds duration with millijoule energy. Further studies should reduce the pulse duration to single picoseconds, using passive modelocking and new techniques for controlling pulse shaping and pulse energy using nonlinear intracavity elements. These new techniques employ refractive index nonlinearities and intracavity aperturing to achieve saturable absorption or saturable gain. If successful, the wavelength tunability and short pulse duration available from this laser system will outperform existing Nd:YAG and Nd:YLF laser technology for a wide range of laser medical applications.

In addition to direct modelocking we are also developing a variable pulse duration, regeneratively amplified titanium-sapphire laser. The 100 fs, 80 MHz, nJ energy Kerr-lens-modelocked oscillator described in a previous section is being incorporated as a seed laser for chirped-pulse regenerative amplification in the flashlamp-pumped titatium-sapphire rod. The completed laser will have variable pulse duration (100 fs - 300 ps), wavelength tunable (700 - 1000 nm) output. Using this source, studies will be performed to correlate tissue incision

---

[49] J.G. Fujimoto, W.Z. Lin, E.P. Ippen, C.A. Puliafito, and R.F. Steinert, "Time Resolved Studies of Nd:YAG Laser Induced Breakdown," *Invest. Ophthal. Vis. Sci.* 26: 1771 (1985); B. Zysset, J.G. Fujimoto, and T.F. Deutsch, "Time Resolved Measurements of Picosecond Optical Breakdown," *Appl. Phys. B.* 48: 139 (1989); B. Zysset, J.G. Fujimoto, C.A. Puliafito, R. Birngruber, and T.F. Deutsch, "Picosecond Optical Breakdown: Tissue Effects and Reduction of Collateral Damage," *Las. Surg. Med.* 9: 193 (1989); D. Stern, R. Schoenlein, C.A. Puliafito, E.T. Dobi, R. Birngruber, and J.G. Fujimoto, "Corneal Ablation by Nanosecond, Picosecond, and Femtosecond Lasers at 532 and 625 nm," *Arch. Ophthalmol.* 107: 587 (1989).

[50] D. Stern, R. Schoenlein, C.A. Puliafito, E.T. Dobi, R. Birngruber, and J.G. Fujimoto, "Corneal Ablation by Nanosecond, Picosecond, and Femtosecond Lasers at 532 and 625 nm," *Arch. Ophthalmol.* 107: 587 (1989).

and collateral injury effects with laser parameters (pulse duration, wavelength, and repetition rate). Studies will include time resolved measurements of the fundamental physical processes in optical breakdown, as well as tissue effects. Special emphasis will be placed on investigating pulse durations shorter than 100 picoseconds in order to reduce the pulse energy needed to achieve optical breakdown below the 70 microjoule level used in our previous study. This system will serve as a valuable and unique tool for optimizing the localizability and incision rate for ultrashort pulse intraocular laser surgery.

1.15.2 Optical Coherence Tomography

Optical coherence tomography (OCT) is a novel non-contact, non-invasive, high resolution tomographic imaging technology that we have developed for the measurement of microstructures in biological tissues.[51] OCT can achieve a spatial resolution of 10 micrometers, which is more than a factor of 10 better than current clinical tomographic imaging modalities such as CT, MRI, or ultrasound B mode imaging. The operation of OCT is analogous to ultrasound imaging. An incident optical beam is reflected or backscattered from tissue structures. The roundtrip delay of the returned light is measured to derive the depth of the reflecting structure. This delay measurement is carried out using an interferometric ranging technique called optical coherence domain reflectometry (OCDR).[52] By incorporating a lateral scanning mechanism to a high speed OCDR system, a two dimensional cross-sectional map of tissue backscattering magnitude is obtained. This data is presented in false-color or gray scale as an optical coherence tomograph. Our OCT studies have concentrated on the measurement of eye structures because the transparency of the ocular media permit easy optical access, and because OCT has the potential of obtaining clinical useful information in very thin eye structures such as the retina and the cornea that are not resolvable using other imaging methods.

This research project spans several different areas including technology development, physical studies, and studies in biological systems *in vitro* and *in vivo*. To address these issues, studies are performed in collaboration with investigators at the Optical Communications Group at MIT Lincoln Laboratory, and the New England Eye Center of the Tufts University School of Medicine.

Our initial results on OCT, published in Science,[53] demonstrated the application of OCT in ophthalmology by performing imaging of the retina *in vitro*. The problem of noninvasive measurement of the retinal thickness and morphology is relevant to the diagnosis of glaucoma and other retinal diseases. In addition, as a example of OCT imaging in a highly scattering system, we have performed studies in coronary arteries *in vitro*.

During the past year, we conducted our first *in vivo* studies of the retinal imaging in human subjects. These OCT images of the retina and the optic nerve head have at least ten times higher depth resolution than conventional ocular imaging methods such as ultrasound, laser scanning tomography, and x-ray computed tomography. These *in vivo* studies were made possible by the development of a high speed OCT system with image acquisition times of several seconds. The OCT system was coupled via a optical fiber and galvanometer driven transverse scanning mechanisms to a slitlamp biomicroscope, a commonly used instrument for clinical examination of the eye. We are continuing to improve the speed and robustness of the system in preparation for clinical studies on glaucoma and other vitreo-retinal diseases. We expect to upgrade the image acquisition time to 1-4 seconds in the near future to minimize patient efforts in clinical studies.

High-resolution imaging of retinal structures is clinically relevant to the diagnosis and management of a variety of retinal diseases such as glaucoma, macular degeneration, macular hole, and macular edema. Non-invasive OCT imaging of retinal structures in human subjects was demonstrated this

---

[51] D. Huang, E.A. Swanson, C.P. Lin, J.S. Schuman, W.G. Stinson, W. Chang, M.R. Hee, T. Flotte, K. Gregory, C.A. Puliafito and J.G. Fujimoto, "Optical Coherence Tomography," *Sci.* 254: 1178 (1991).

[52] R.C. Youngquist, S. Carr, and D.E.N. Davies, "Optical Coherence-domain Reflectometry: a New Optical Evaluation Technique," *Opt. Lett.* 12: 158 (1987); K. Takada, I. Yokohama, K. Chida, and J. Noda, "New Measurement System for Fault Location in Optical Waveguide Devices Based on an Interferometric Technique," Appl. Opt. 26: 1603 (1987); D. Huang, J. Wang, C.P. Lin, C.A. Puliafito and J.G. Fujimoto, "Micron-resolution Ranging of Cornea Anterior Chamber by Optical Reflectometry," *Lasers Surg. Med.* 11: 419 (1991); E.A. Swanson, D. Huang, M.R. Hee, J.G. Fujimoto, C.P. Lin, and C.A. Puliafito, "High-speed Optical Coherence Domain Reflectometry," *Opt. Lett.* 17: 151 (1992).

[53] D. Huang, E.A. Swanson, C.P. Lin, J.S. Schuman, W.G. Stinson, W. Chang, M.R. Hee, T. Flotte, K. Gregory, C.A. Puliafito and J.G. Fujimoto, "Optical Coherence Tomography," *Sci.* 254: 1178 (1991).

year. These tomographs have far higher resolution than other non-invasive imaging techniques and, to our knowledge, are the first images that actually allow one to delineate retinal layers *in vivo*.

In OCT images of the foveal region of the retina, the retina layers were identifiable from the previously known anatomy. The backscattering is very weak from the foveolar region, where the retina consists mainly of the photoreceptor layer and the Henle fiber layer. This contrasts with the surrounding region, where the brighter nerve fiber layer and the plexiform layers of the retina appear to gradually increase in thickness further from the center of the fovea. Other posterior eye structures such as the vitreous medium, the choroid, and the sclera, are also clearly identifiable. The ability of OCT to image these retinal structural details demonstrates its potential in the diagnosis and quantitative monitoring of retinal diseases such as macular degeneration, macular hole, and macular edema.

In OCT images of the retina around the optic nerve head, the retinal nerve fiber layer (RNFL), appear as a thick, highly scattering layer in the inner retina that contrasts with the subjacent retinal layers. Accurate RNFL thickness measurements are relevant to the diagnosis and management of glaucoma.[54] Glaucoma, where elevated intraocular pressure produces retinal nerve fiber atrophy, is a leading cause of blindness. The diagnosis of glaucoma is a difficult clinical problem. Intraocular pressure measurements do not reliably predict disease progression. Other diagnostic parameters such as visual field defects and optic disc cupping are detectable only after significant (~ 50 %) loss in the retinal nerve fiber layer (RNFL) has already occured. Because both medical and surgical treatments for glaucoma can cause substantial adverse effects, there is a great deal of uncertainty and dilemma in making early treatment decisions. Early detection of optic nerve fiber atrophy with OCT could greatly reduce this uncertainty. Further trials in glaucoma patients and glaucoma animal models will determine whether OCT measurements can provide early criteria by which to make treatment decisions in glaucoma patients.

1.15.3 Transillumination Imaging

Optical transillumination imaging of tissue offers the potential of a non-invasive diagnostic with non-ionizing radiation and the possibility of using spectroscopic properties to distinguish tissue pathology and probe metabolic function. Optical transillumination is analogous to x-ray imaging; however, optical radiation is relatively safe and can provide tissue contrast based on spectroscopic differences. Unfortunately, absorption and multiple light scattering severely limit optical image resolution in dense or thick tissue specimens. Recently, there has been interest in transillumination as an alternative or supplement to mammography for early breast tumor detection. Optical radiation may be capable of distinguishing malignant tissue without the hazards of x-ray imaging based on the optical properties of the surrounding tumor neovascularization.

Several time or spatially resolved optical imaging techniques have been proposed which reduce image degradation due to scattering by discriminating against the spatial or temporal characteristics of scattered light. Spatially resolved methods, based on the confocal imaging principle, require detected light to have a certain directionality or spatial phase coherence.[55] Time resolved techniques rely on the fact that multiply scattered light travels a longer path through tissue compared to unscattered light, and therefore may be rejected temporally. A short pulse propagating through a scattering media will be severely lengthened due to scattering, but a shadowgram of hidden objects may be reconstructed by temporally isolating the earliest arriving, least scattered component of the transmitted light from the later-arriving diffuse, or multiply scattered light. Any of a number of different incoherent or coherent imaging techniques may be used to time-gate early arriving light, including streak camera imaging,[56] photon

---

[54] H.A. Quigley and E.M Addicks, "Quantitative Studies of Retinal Nerve Fiber Layer Defects," *Arch. Opthalmol.* 100: 807 (1982).

[55] M. Toida, M. Kondo, T. Ichimura, and H. Inaba, "Two-Dimensional Coherent Detection Imaging in Multiple Scattering Media Based on the Directional Resolution Capability of the Optical Heterodyne Method," *Appl. Phys. B* 52: 391-394 (1991); D.S. Dilworth, E.N. Leith, and J.L. Lopez, "Imaging Absorbing Structures Within Thick Diffusing Media," *Appl. Opt.* 29: 691-698 (1990).

[56] K.M. Yoo, B.B. Das, and R.R. Alfano, "Imaging of a Translucent Object Hidden in a Highly Scattering Medium from the Early Portion of the Diffuse Component of a Transmitted Ultrafast Laser Pulse," *Opt. Lett.* 17: 958-960 (1992); J.C. Hebden, R.A. Kruger, and K.S. Wong, "Time Resolved Imaging Through a Highly Scattering Medium," *Appl. Opt.* 30: 788-794 (1991).

counting,[57] nonlinear gating,[58] and time-resolved interferometry[59] or holography.[60]

In collaboration with MIT Lincoln Laboratory, we have developed a new technique for time-gated imaging through turbid media based on optical coherence tomography (OCT).[61] In femtosecond transillumination optical coherence tomography, femtosecond pulses and coherent heterodyne detection time-resolve transmitted light based on its coherence properties.[62] The operation principle of transillumination OCT is analogous to reflection-mode OCT; however, instead of depth resolving reflected light, the coherence properties of transmitted light are used to transversely resolve objects otherwise obscured by multiple scattering. Short pulses (50 to 400 fs) from a Kerr-lens modelocked $Ti:Al_2O_3$ laser are used in conjunction with a modified fiber-optic Mach-Zehnder interferometer. A fiber beamsplitter divides the incident pulses into a reference delay path and a sample transmission path. Light retroreflected from the variable delay reference mirror is recombined with temporally broadened light transmitted through the sample at another fiber splitter and is incident on a photodetector. Interference signal is created at the detector only for the coherent component of the transmitted pulse which temporally overlaps the reference pulse. Using dual balanced detectors to reduce excess laser noise in conjunction with lock-in amplification, we achieve the quantum shot noise detection limit. The transillumination system can resolve transmitted light as weak as 5 femtowatts, which is 10^{-13} of the incident optical power of 50 mW (a 130 dB dynamic range).

To study the basic characteristics of coherent photon migration through scattering media, we have used transillumination OCT to temporally profile the coherent constituent of the on-axis scattered pulse propagating through suspensions of uniform scattering microspheres. Similar to earlier studies of incoherent migration,[63] the coherent transmitted light consists of an unscattered ballistic component, and a later arriving, temporally broadened diffuse component. The arrival time and temporal profile of these components have been investigated as functions of scattering anisotropy and microsphere concentration, and have been qualitatively correlated with predictions from Mie scattering theory. Compared to previous studies of incoherent photon migration, the coherent diffuse component displays a reduced temporal extent due to loss of phase coherence with multiple scattering. The ballistic peak power attenuates exponentially as the number of scattering mean-free-paths (MFPs) contained in the scattering medium, or equivalent sample thickness. The transmitted diffuse power dominates ballistic light for sample thicker than about 25 scattering MFPs, fairly independent of scattering anisotropy. The diffuse power also attenuates about a factor of 10 more slowly in the exponential with increasing sample thickness.

Time-gated imaging of hidden objects embedded in scattering media is achieved by fixing the reference arm path length and raster scanning the sample to create a two-dimensional image of interference signal magnitude. High resolution (100 μm) images of an Air Force resolution chart placed in the center of a 1 μm diameter microsphere suspension 27 scattering MFPs thick have been obtained by using

---

[57] S. Andersson-Engels, R. Berg, S. Svanberg, and O. Jarlman, "Time-resolved Transillumination for Medical Diagnostics," *Opt. Lett.* 15: 1179-1181 (1990).

[58] L. Wang, P.P. Ho, C. Liu, G. Zhang, and R.R. Alfano, "Ballistic 2-D Imaging Through Scattering Walls Using and Ultrafast Optical Kerr Gate," *Sci.* 253: 769-771 (1991); K.M. Yoo, Q. Xing, and R.R. Alfano, "Imaging Objects Hidden in Highly Scattering Media Using Femtosecond Second-harmonic-generation Cross-correlation Time Gating," *Opt. Lett.* 16: 1019-1021 (1991); M.D. Duncan, R. Mahon, L.L. Tankersley, and J. Reintjes, "Time-gated Imaging Through Scattering Media Using Stimulated Raman Amplification," *Opt. Lett.* 16: 1868-1870 (1991).

[59] D. Huang, E.A. Swanson, C.P. Lin, J.S. Schuman, W.G. Stinson, W. Chang, M.R. Hee, T. Flotte, K. Gregory, C.A. Puliafito and J.G. Fujimoto, "Optical Coherence Tomography," *Sci.* 254: 1178 (1991).

[60] K.G. Spears, J. Serafin, N.H. Abramson, X. Zhu, and H. Bjelkhagen, "Chrono-Coherent Imaging for Medicine," IEEE Trans. *Biomed. Engr.* 36: 1210-1221 (1989); E. Leith, H. Chen, Y. Chen, D. Dilworth, J. Lopez, R. Masri, J. Rudd, and J. Valdmanis, "Electronic Holography and Speckle Methods for Imaging Through Tissue Using Femtosecond Gated Pulses," *Appl. Opt.* 30: 4204-4210 (1991).

[61] D. Huang, E.A. Swanson, C.P. Lin, J.S. Schuman, W.G. Stinson, W. Chang, M.R. Hee, T. Flotte, K. Gregory, C.A. Puliafito, and J.G. Fujimoto, "Optical Coherence Tomography," *Sci.* 254: 1178 (1991).

[62] M.R. Hee, J.A. Izatt, J.M. Jacobson, E.A. Swanson, and J.G. Fujimoto, "Femtosecond Transillumination Optical Coherence Tomography," *Opt. Lett.*, forthcoming.

[63] Y. Kuga, A. Ishimaru, and A.P. Bruckner, "Experiments on Picosecond Pulse Propagation in a Diffuse Medium," *J. Opt. Soc. Am.* 73: 1812-1815 (1983); K.M. Yoo and R.R. Alfano, "Time-resolved Coherent and Incoherent Components of Forward Light Scattering in Random Media," *Opt. Lett.* 15: 320-322 (1990).

transillumination OCT to coherence-gate only the early arriving ballistic component of the transmitted light. Since ballistic light is unscattered, the spatial resolution of ballistic gated imaging is theoretically diffraction limited. However, imaging with ballistic light is virtually impossible through thick specimens due to the exponential attenuation of the ballistic component with sample thickness. We have derived a fundamental ballistic imaging thickness limit for any optical imaging technique based on quantum noise considerations and optical tissue damage thresholds. For parameters required for early breast tumor detection, this thickness limit evaluates to approximately 4 mm breast tissue.

The combined temporal and directional rejection of scattered light with transillumination OCT allows a comparison of time and spatially resolved imaging techniques. A purely spatial discrimination technique, such as confocal imaging, will be sensitive to the transillumination OCT interference signal integrated over all coherence-gate delays. Studies of time-resolved photon migration with confocal imaging show that ballistic imaging is impossible for spatially resolved methods because a substantial amount of late arriving diffuse light may be coherent at the detector when the sample is thicker than about 20 scattering MFPs.

Since ballistic imaging is restricted to relatively thin samples, medically relevant applications require gating the early arriving portion of the diffuse transmitted light. Spatial resolution is sacrificed for the wider coherence-gate delays necessary to image through thick samples. We characterized the degradation in resolution versus coherent photon arrival time for various sized opaque bars placed in 25 scattering MFPs of 1 μm diameter microspheres. The spatial resolution for a given transit delay was found to be bounded above by a simple square-root limit, obtained from geometric considerations, and below by an empirically derived linear limit. Consideration of these limits enabled us to design a transillumination OCT system capable of resolving a 1 mm width resolution chart embedded in 1.5 cm chicken breast *in vitro*. To our knowledge, this image represents the thickest biological sample with similar scattering characteristics through which submillimeter image resolution has been obtained.

The fundamental resolution and thickness limits we have identified in these basic studies should prove useful in the design of future time-domain imaging techniques for biomedical applications.

1.16 Observation of Gain in Ni-like Nb

Sponsors

Bose Corporation
Lawrence Livermore National Laboratories
Subcontract B160530
U.S. Department of Energy
Grant DE-FG02-89-ER14012

Project Staff

Professor Peter L. Hagelstein, Dr. Santanu Basu, James G. Goodberlet, Sumanth Kaushik, Martin H. Muendel

During the past four years, we have assembled an experimental facility suitable for testing various novel and low power approaches to EUV and soft x-ray lasers.[64] Our facility consists of a Nd:YLF oscillator and Nd:glass pre-amplifier (currently being upgraded to a Nd:YLF pre-amplifier), a zig-zag slab power amplifier, a 200-liter vacuum chamber with an internal target positioning and alignment system, and two EUV spectrometers. Various components of our facility have been described in previous annual *RLE Progress Reports.*

Last spring we began taking data, searching for the laser line in Ni-like Mo. The principal diagnostic for this work is a nearly stigmatic spectrometer which is based on a near-normal incidence spherical grating which images onto the cathode of a streak camera as illustrated below in figure 1. The grating was loaned by the National Research Laboratory (NRL); the streak camera was loaned by Lawrence Livermore National Laboratories.

The principal laser lines in mid-Z Ni-like ions have not been previously identified, and as a result we have relied on theory to a significant degree to guide our search. The computation of accurate line positions for the $3d^9 4d\ ^1S - 3d^9 4p\ ^1P$ transition is hindered by strong correlation effects due to mixing between the upper laser state and the $4d^{10}\ ^1S$ ground state. For example, the results of a multi-configuration Hartree-Fock calculation gives the wavelength of the line in Ni-like Mo to be near 172 Å; the correlation corrections bring the wavelength near 190 Å, a correction of about ten percent. We first corrected the wavelength using data from Eu obtained by Lawrence Livermore National Laboratories, which led to an interpolated wavelength of 194

[64] P.L. Hagelstein, "Short Wavelength Lasers: Something Old Something New," *Proceedings of the OSA meeting on Short Wavelength Coherent Radiation: Generation and Applications,* ed. R.W. Falcone and J. Kirz, 1988.

Å. This value was updated using a low-Z measurement in As to provide a further correction to 191 Å. In the spring of 1992, a measurement of the analog line in Ni-like Sn was reported by the NRL at 119.1 Å; we were able to use this value to improve our prediction to 188.8 Å for Mo. When we finally found the laser line in Ni-like Mo, it appeared at 189.2 Å, as shown in figure 2.

The efficiency of the NRL grating becomes quite low at wavelengths below 200 Å, and this poor efficiency hindered our experiments; many shots would be required to find the nearby strong Cu-like lines, and the laser line would appear after only the most heroic efforts. As a result, we decided to shift the primary focus of our experiments to a study of gain in Ni-like Nb, which was predicted to occur at

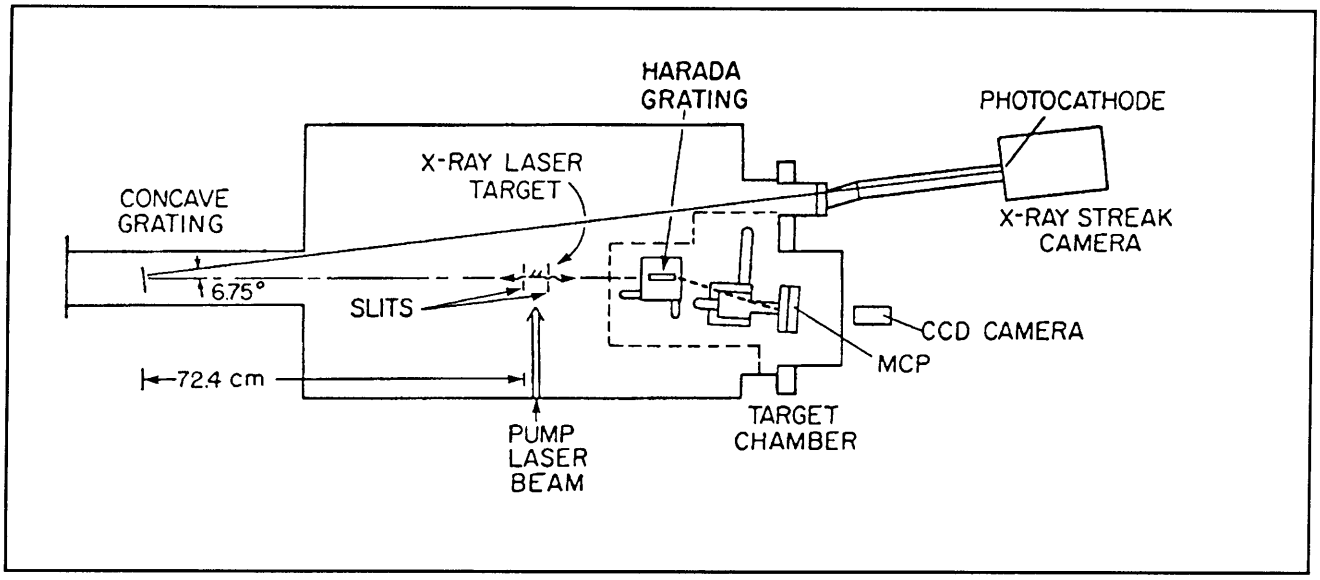

Figure 1. Schematic of the x-ray laser target chamber and spectrometers.

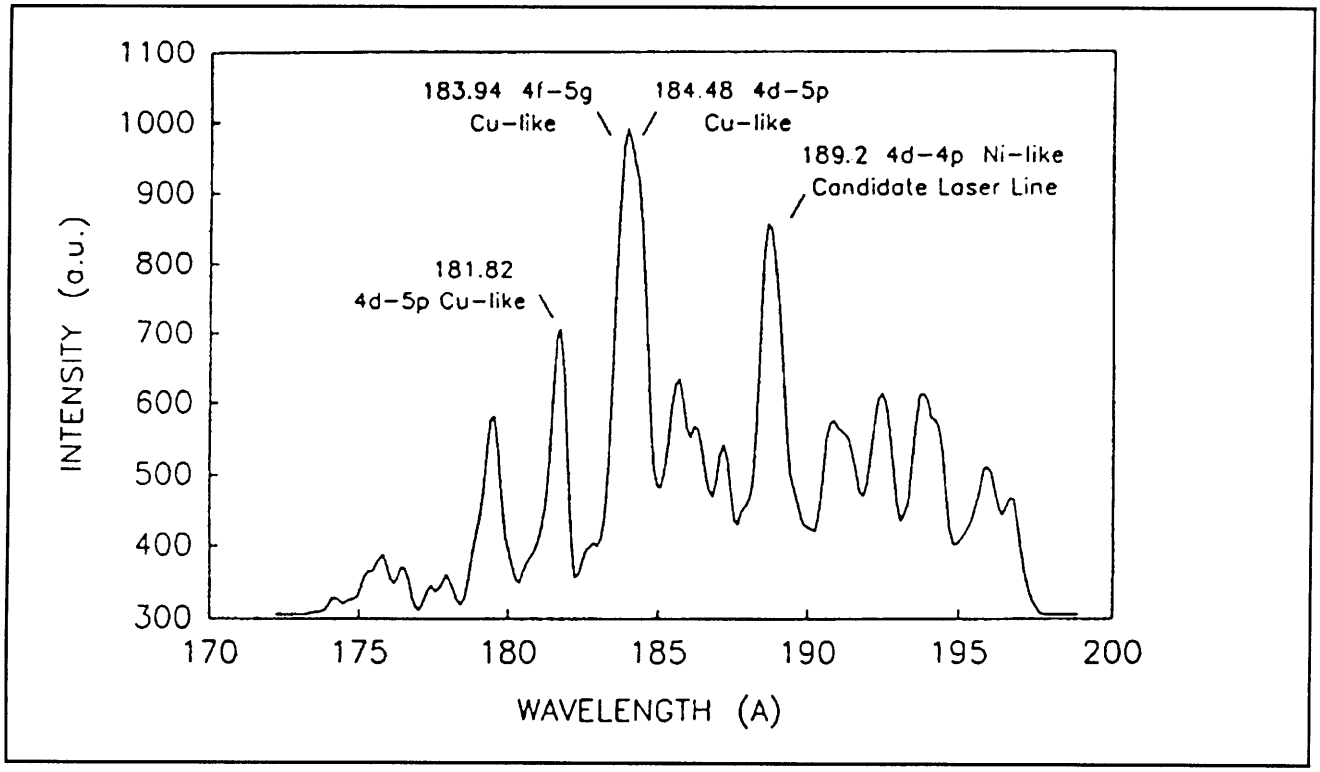

Figure 2. Spectrum of Mo in the vicinity of the Ni-like Mo $3d^9 4d\ ^1S - 3d^9 4p\ ^1P$ laser line.

203.7 Å. The transition in Nb was readily found, and it occured at a wavelength of 204.2 Å.

The principal laser lines in Ni-like ions are quite weak if no gain is present. Since we observed the lines, and since we were able to make the candidate laser line dominate the spectrum locally, we knew that we had produced significant gain. This fact is important, because previously gain in Ni-like ions had only been produced at larger laser facilities in experiments involving kilojoules of incident laser pump energy; in our experiments we used less than 1 joule per pump pulse. Our result constituted a rather major breakthrough in the area of collisionally-driven EUV and soft x-ray lasers.

It remained to quantify the small signal laser gain. Experiments were conducted in which the beam was blocked to produce various plasma amplifier lengths, and the resulting measured intensity was plotted as a function of the amplifier length. The resulting curve shows exponentiation characteristic of laser gain, with a corresponding gain coefficient of about 3 cm^{-1}, as shown in figure 3. To date, out best data has been taken at a length of 9.1 mm, using about 1 joule per pulse of pump energy. The resulting spectra, shown in figure 4, is characteristic of between 3.0-3.5 total gain-lengths.

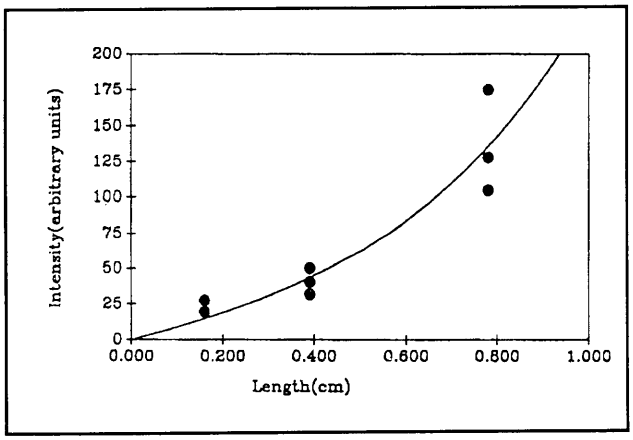

Figure 3. Intensity as a function of length for the Ni-like Nb $3d^9 4d\ ^1S - 3d^9 4p\ ^1P$ laser line.

Publications

Basu, S., et al, presented at LEOS, Boston, Massachusetts, November 1992.

Basu, S., P.L. Hagelstein, J.G. Goodberlet, M.H. Muendel, and S. Kaushik. "Amplification in Ni-like Nb at 204 Å Pumped by a Tabletop Laser." Submitted to *Appl. Phys. B.*

Hagelstein, P.L. "Short Wavelength Laser Studies at MIT: An Update." In *Solid State Lasers III.* Ed. G.J. Quarles. *Proc. SPIE.* 1627: 340 (1992).

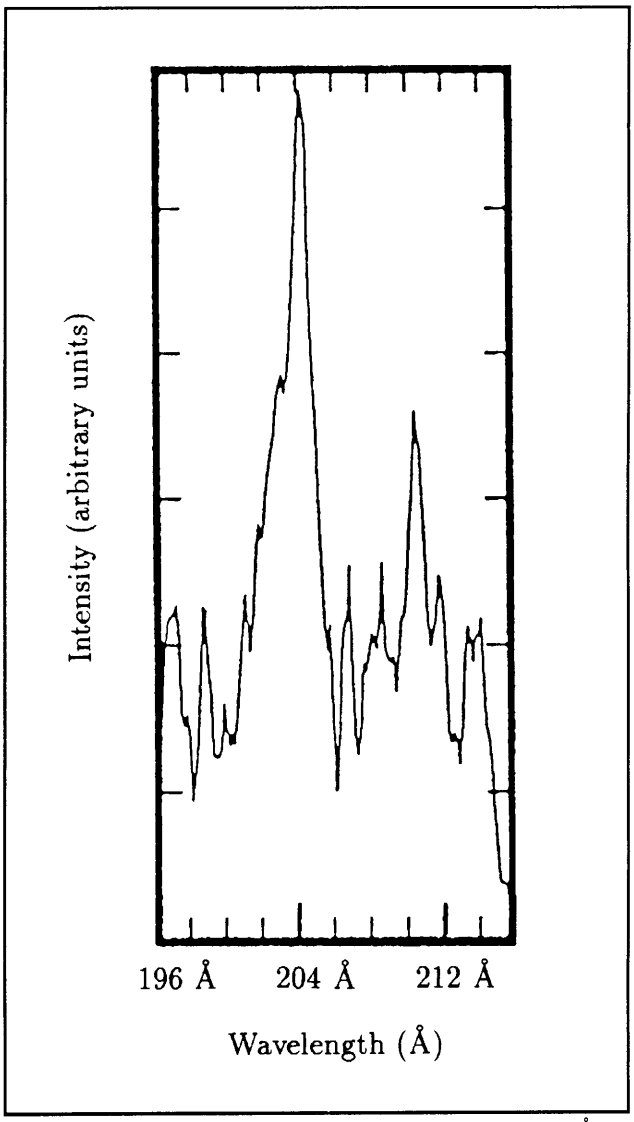

Figure 4. The $3d^9 4d\ ^1S - 3d^9 4p\ ^1P$ laser line (204.3 Å) in Ni-like Nb at 9.1 mm.

1.17 Pump Pulse Length

Project Staff

James G. Goodberlet, Professor Peter L. Hagelstein

We lost a Nd:glass preamplifier rod due to optical damage in November, and this loss has caused downtime. We took the opportunity to upgrade the preamplifier to a Nd:YLF rod, but before coming back up to run integral EUV laser experiments, we wanted to check the pulselength to make certain that the oscillator was not producing short pulses

spuriously. According to specifications, the Lumonics oscillator is supposed to provide 70 psec pulses; significantly shorter pulses at full energy could potentially damage the system.

To investigate this issue, autocorrelation of the electric field was accomplished using a Michaelson interferometer with tilted mirrors to produce noncollinear interfering beams at the detector. If the pulses arrive at the detector coincidently, they produce an intereference pattern; additional path length in one arm produces a delay which can reduce or destroy the interference.

The initial results of the interferometry indicated that some of the pulses produced by the oscillator were as short as 25 psec. A weakness of an autocorrelator based on field rather than intensity is that it does not distinguish between a short pulse and a chirped pulse; inspection of the second harmonic signal from a KDP crystal indicated that indeed short pulses were present.

The large variation in pulse length was found to be due to an absence of prelase signal before the oscillator Q-switched; the Lumonics laser was originally shipped and brought up at MIT with Lumonics staff to operate without prelasing. We reset the oscillator to prelase before Q-switching which stabilized the system.

Intensity autocorrelation was performed on the oscillator output, and the resulting pulses were determined to be near 60 psec; an etalon was acquired which results in 120 psec pulses.

In light of these results, some of the experimental difficulties which had been noted were likely due to the substantial pulse variability that was present in the system. A question now arises whether the best data that we obtained which showed gain occured because the pump pulse was short, following from the increased intensity present. If so, this will limit how much more EUV laser total gain we will be able to obtain in the future. The dependence of gain on pulse length will be the focus of experiments to take place in the coming months.

1.18 End-pumped X-ray Lasers

Sponsors

Bose Corporation
Lawrence Livermore National Laboratories
Contract B160530
U.S. Department of Energy
Grant DE-FG02-89-ER14012

Project Staff

Professor Peter L. Hagelstein, Dr. Santanu Basu, Martin Muendel

Our research has recently led to a novel and very efficient EUV amplifier which is able to obtain 1 gain-length at 204 Å per 0.3 joules of incident 1μ pump energy; previous experimental work using collisional excitation schemes in this wavelength range has involved relative pumping efficiencies measured in gain-lengths per kilojoule.

The improvements which we have obtained are due primarily to: (1) the use of Ni-like ions, which has not previously been explored in this wavelength range; and (2) the use of a pulse train to create and then pump the plasma, which results in a very low ion temperature with an associated high gain due to a reduction in Doppler broadening.

The question arises as to whether further improvements might lead to still more gains in efficiency. For example, most of the laser energy which is absorbed goes ultimately into hydrodynamic kinetic energy or simply heats high density material far away from where gain is produced. Only about one part in 10^4 of the absorbed pump energy is ultimately utilized for the production of gain.

We have considered possible approaches towards improving the efficiency of EUV and soft x-ray laser amplifiers. If a pre-expanded low density (around 10^{19} electrons/cm^3) plasma amplifier could be produced, then laser energy absorbed at low density would be used more efficiently to produce gain (the conversion efficiency of laser light to hydrodynamic energy in such a plasma is very poor). But such a scheme is ill-suited to current x-ray laser pumping arrangements since the absorption coefficient of a low density plasma is very low; less than one percent of the pump radiation would be absorbed in a 100 μ wide low density plasma pumped from the side under conditions where gain would be expected.

A potential solution to this problem is to modify the pumping geometry and to pump from the end instead of the side. Ideally, the pump radiation would in this case be absorbed where it does the most good, and the EUV beam builds up as it copropagates with the optical beam. The total number of gain lengths produced before the beam is completely absorbed will determine whether the approach is a good one.

The effectiveness of this approach can be seen by comparing the total number of EUV gain lengths gL with the number of inverse Bremsstrahlung absorption lengths $\kappa_{ib}L$. Interestingly enough, this ratio is maximized at low density. Normally, x-ray laser

designers seek to maximize the small signal gain in a laser design; in this case the total number of gain-lengths is maximized at a small signal gain which is less than the maximum possible small signal gain.

At an electron density which is low compared to the critical density ($N_e \ll N_c$), and also low compared to the characteristic density of the laser transition ($N_e \ll A_u / \langle \overline{\sigma v} \rangle_u$), the ratio of the EUV gain to IR absorption becomes essentially independent of electron density. It can be shown that the low density limit is given by

$$\frac{gL}{\kappa_{ib}L} = \sigma_{SE} \frac{N_o}{N_e} \frac{\langle \overline{\sigma v} \rangle_{uo}}{A_u} \frac{4}{3} \sqrt{\frac{\pi}{2}} \frac{c^3 (mkT_e)^{3/2}}{Z^* e^6 \ln \Lambda \lambda^2} (1 - \zeta)$$

In this formula, σ_{SE} is the stimulated emission cross section, N_o is the ground state $3d^{10}\,{}^1S$ population, $\langle \overline{\sigma v} \rangle_{uo}$ is the rate coefficient for excitations from the ground state to the upper state, Z^* is the average ionization charge assuming a single element plasma, and $(1 - \zeta)$ is the ratio of the inversion density to the upper laser state density at low electron density. In the case of a low density Ni-like Mo EUV amplifier, this ratio can be larger than 100.

The implication of this result is that it should be possible in principle to obtain further very large improvements in the efficiency of EUV and soft x-ray lasers through the successful development of end-pumped lasers.

A primary technical drawback of such pumping schemes is that the pump laser will either refract or diffract out of the plasma amplifier before any significant fraction of the beam energy is absorbed in a real system unless some way can be found to keep the pump beam in the plasma. It is natural to consider a "soda-straw" type geometry; unfortunately, such a system by necessity brings high density plasma and the associated hydrodynamic losses in close proximity to the plasma amplifier.

We have therefore considered pumping schemes that involve segmented amplifiers wherein external optical components are used to help refocus the beam following transmission through individual segments. Examples of such schemes are shown in figures 5-7.

Publication

Hagelstein, P.L., S. Basu, and M. Muendel. "XRL Research at MIT: Recent Progress." *Proceedings of the Third International Conference on X-ray Lasers,* Schliersee, Germany, May 1992.

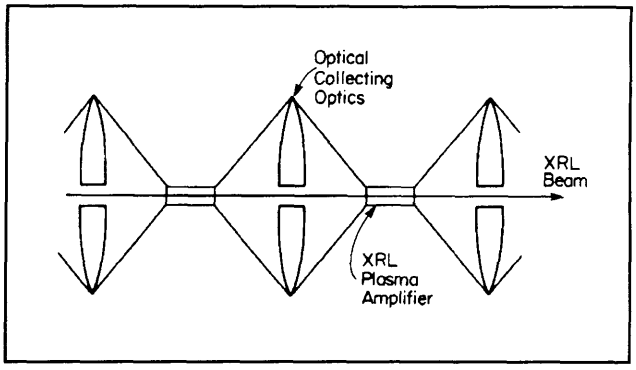

Figure 5. Schematic of a simple stable end-pumped laser.

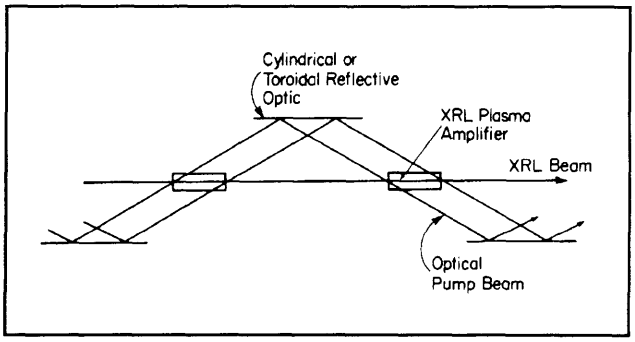

Figure 6. Schematic of a zig-zag end-pumped laser.

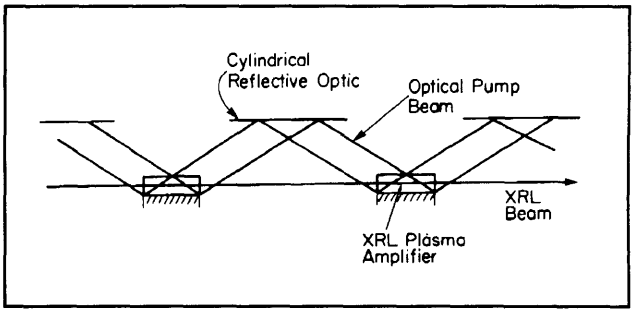

Figure 7. Schematic of solid surface targets pumped in sequence.

1.19 The Kinetics and Hydrodynamics of Laser-Generated Plasmas

Sponsor

MIT Lincoln Laboratory

Project Staff

Professor Peter L. Hagelstein, Ann W. Morgenthaler, Janet L. Pan

Laser-produced plasmas which are ablated from the surface of a solid are currently being used for x-ray laser amplifiers in a number of laboratories around

the world; our group at MIT has been focusing on the use of such plasmas primarily for collisional (Ni-like) x-ray lasers as described elsewhere in this report.

The success of the collisional scheme depends strongly on achieving a high electron temperature in the low-density coronal region of the plasma. The laser light is absorbed primarily near the critical surface (at 10^{21} electrons/cm^3 for 1 μm pump radiation), where the electron temperature is determined by a balance between inverse Bremsstrahlung absorption and flux-limited thermal conduction in other parts of the plasma. The thermal conductivity is a strongly increasing function of the electron temperature, and it is expected that once a high temperature is established near the critical surface, heating of the low density corona by conduction will quickly follow.

A basic understanding of electron thermal conduction in the plasma is therefore critical for making a quantitative prediction of the electron temperature as a function of the pump laser intensity, especially in regimes where significant flux limiting occurs. This has motivated our interest in the basic physics of electron transport in laser-produced plasmas. The approach which we have explored involves taking moments of the full, collisional Boltzmann equation, with Coulombic collisions described by the Landau operator as outlined in last year's *RLE Progress Report.* The treatment of collisions in the moment method is technically complicated, and we have recently reported a rather general solution to this problem that is amenable to numerical modeling.[65] Exact analytic coupling coefficients describing the interaction between identical particles during a collision are a central result of this paper, and this work has been extended to describe arbitrary collisions between unlike particles (e.g., electron-ion collisions) which are critical for describing plasma interactions.

The end result of the moment method is a set of coupled equations describing average plasma quantities such as density, mean velocity, temperature, and heat flux. The simplest useful set of such coupled equations are those describing electrons and ions in a 1 1/2 dimensional model (1-D space and 2-D velocity). The time-evolution equations for the lowest order moments are mass continuity equations:

$$\frac{\partial}{\partial t} N_e + \frac{\partial}{\partial z} (N_e v_e) = 0 \tag{1}$$

$$\frac{\partial}{\partial t} N_i + \frac{\partial}{\partial z} (N_i v_i) = 0 \tag{2}$$

where N_e and N_i are electron and ion densities, and v_e and v_i are average $\hat{z}$-directed electron and ion velocities. The first order moments give rise to momentum equations

$$mN_e \frac{\partial v_e}{\partial t} + mN_e v_e \frac{\partial v_e}{\partial z} + eEN_e + \frac{\partial (N_e T_e)}{\partial z} = -\frac{4\sqrt{2\pi}\ \ln \Lambda Z^2 e^4 N_e N_i m^{1/2}}{3T_e^{3/2}} (v_e - v_i) \tag{3}$$

$$MN_i \frac{\partial v_i}{\partial t} + MN_i v_i \frac{\partial v_i}{\partial z} - ZeEN_i + \frac{\partial (N_i T_i)}{\partial z} = +\frac{4\sqrt{2\pi}\ \ln \Lambda Z^2 e^4 N_e N_i m^{1/2}}{3T_e^{3/2}} (v_e - v_i) \tag{4}$$

Here, T_e and T_i are electron and ion temperatures, *m* and *M* are electron an ion masses, *Z* is the average ionic charge of the plasma, and $\ln \Lambda$ is the electron-ion Coulomb logarithm. A final set of equations describes the temperature evolution of this plasma:

$$3N_e \frac{\partial T_e}{\partial t} + 3N_e v_e \frac{\partial T_e}{\partial z} + 2N_e T_e \frac{\partial v_e}{\partial z} + \kappa \frac{\partial^2 T_e}{\partial z^2} = -\frac{8\sqrt{2\pi}\ \ln \Lambda Z^2 e^4 N_e N_i m^{1/2}}{MT_e^{3/2}} (T_e - T_i) \tag{5}$$

$$3N_i \frac{\partial T_i}{\partial t} + 3N_i v_i \frac{\partial T_i}{\partial z} + 2N_i T_i \frac{\partial v_i}{\partial z} = +\frac{8\sqrt{2\pi}\ \ln \Lambda Z^2 e^4 N_e N_i m^{1/2}}{MT_e^{3/2}} (T_e - T_i) \tag{6}$$

---

[65] A.W. Morgenthaler and P.L. Hagelstein, "Kinetic Theory of a Non-Equilibrium Plasma: Evaluation of the Vectorized Collisional Boltzmann Equation," submitted to *Phys. Fluids B.*

where the linearized thermal conductivity κ can be derived to arbitrary accuracy from the higher-order moment equations for this simplest plasma. The heat conduction term in (5) is the place where the higher order moments couple to the temperature equation, and by considering sufficient numbers of higher-order moments, thermal flux limitation should appear quite directly.

It appears that the plasma hydrodynamic equations have many similarities with the equations governing drift and diffusion in semi-conductors; therefore, we will attempt to numerically solve the moment equations with efficient techniques such as Gummel's method. The equations governing electron and ion motion are not typically solved in this coupled form, and our goal is to produce numerical models of a laser-generated plasma which may be useful design tools for further developments of the x-ray laser. We are also interested in quasi-analytic models of plasma heating by intense electric fields, which can be found by considering fast and slow variations of all field quantities. A simple model describing the coupling of electromagnetic fields into the plasma is currently under investigation.

Because the "machinery" developed for understanding laser plasma kinetics is sufficiently general, we should be able to apply our techniques to other outstanding problems in plasma physics.

1.20 An Analytical Solution of the 2D Exciton-Phonon Matrix Element

Project Staff

Sumanth Kaushik, Professor Peter L. Hagelstein

Work has been on the development of analytical and numerical methods for the *ab initio* absorption lineshapes in two dimensional systems. We have focused our attention of multiple quantum well structures (MQW) for which considerable amount of experimental data exist in the literature. The in-plane confinement of the electron and hole due to the quantum wells enable these devices, even at room temperatures, to exhibit pronounced excitonic effects which can be strongly modified by optical and electro-optical modulation.

An important parameter that characterizes the strength of excitonic effects is the absorption linewidth. The sharper the linewidth, the more pronounced are the excitonic effects. At room temperatures, the dominant contribution to the linewidth is the interaction of the quasi two-dimensional excitons with optical phonons. Various theoretical models exist in the field to calculate the phonon contribution to the absorption linewidth. However, in all these models, a fundamental quantity needed in the computation is the photon/phonon matrix element

$$\langle \lambda, m | \exp(iq \bullet r) | 0,0 \rangle \sim I$$

between the ground state and an arbitrary excited state of the exciton.

Often, for convenience, the exciton is modeled as a two-dimensional hydrogen atom where the parameters such as the Bohr radius and the binding energy are adjusted so as to reproduce more exact calculations. In the limit where the initial and final states are 2D hydrogen states, the above matrix element can be evaluated analytically. However, in evaluating this matrix element, one encounters an integral transform of the form

$$I \equiv \int_0^\infty x(bx)^\nu \exp(-px)\,{}_1F_1(a,2\nu+1,bx)J_\nu(\gamma x)dx$$

where *a,b,p* are complex and ν, γ are real. In the particular case of the matrix element the parameters are defined to be $b=1/2\lambda$, $\nu = |m|$ and $p=1+1/4\lambda$ with *m* being an integer and λ being either real (for bound-bound transitions) or complex (for bound-free transitions).

We have managed to formulate an analytical solution to this matrix element which is written in the form

$$I = (\pm)\Gamma(2\nu+1)\left(\frac{z^3}{p^2}\right)\xi^{-a+\nu-1} \times$$

$$\left[(2\nu+1-2a)\xi P^{-\nu}_{-a+\nu}(\rho) - a\left(2-\frac{b}{p}\right)P^{-\nu}_{-a+\nu-1}(\rho)\right]$$

where the *a,b,p* are arbitrary and complex and ν, γ are arbitrary and real and the parameters. This matrix element, in addition to enabling rapid computation of lineshape, enables one to develop very useful and simple scaling relations for the linewidth in term of phonon coupling and well parameters.

Publications

Kaushik, S., and P.L. Hagelstein. "A Semi-empirical Line Shape Model of GaAs MQW Structures." Submitted to *IEEE J. Quantum Electron.*

Kaushik, S. "An Analytical Solution to the 2-D Exciton-Phonon Matrix Element." Submitted to *J. Math. Phys.*

1.21 Quantum Dot Diode Lasers

Sponsors

MIT Lincoln Laboratory
Rockwell International Corporation

Project Staff

Janet L. Pan

Lasers in the thermal infrared (2 to 10 micrometer) wavelength regime are useful for spectroscopy, medicine, and fiber optics. For medicinal purposes, these lasers take advantage of the large absorption of water in various windows in the thermal infrared. For spectroscopy, these lasers are useful because many substances (such as organic molecules or pollutants in the air) have characteristic vibrational frequencies in the thermal infrared.

We are interested in quantum dots for improving semiconductor lasers in the thermal infrared. In this wavelength regime, the Auger rate limits the performance of conventional semiconductor lasers,[66] such as the lead salt semiconductor lasers, to low temperatures. Quantum dots, with their discrete energy levels, could greatly reduce the Auger rate. We have calculated interband Auger processes in quantum dots,[67] and have shown that the use of large potential barriers surrounding quantum dots could greatly reduce the Auger rates in quantum dot lasers over those in conventional semiconductor lasers.

Figure 8 shows the temperature dependence of the CCCV and CVVV intraband Auger lifetimes for a 150 Å radius InSb quantum dot (with a bandgap at 4.8 micrometers (258 meV)) surrounded by CdTe barriers. We found that enough Auger processes were excluded by the large CdTe potential barriers so that our InSb quantum dot room temperature Auger lifetime was about 135 nanoseconds. This is to be compared with the calculated Auger rates for other semiconductors with band gaps in the infrared. For GaSb with a bandgap of 670 meV (1.8 micrometers), the Auger lifetime at 77 K for a carrier concentration in the bulk of $\frac{2}{\frac{4}{3}\pi R^3}$ was calculated[68] to be about 0.01 nanoseconds and measured[68] to be about 1 nanosecond for our volume of $\frac{4}{3}\pi(150\text{Å})^3$. A 4.5 nanosecond Auger lifetime[69] was found at liquid nitrogen temperature for a conventional 10 μm $Pb_{0.82}Sn_{0.18}Te$ laser, whose active region injected carrier concentration is $0.8 \times 10^{17}cm^{-3}$ or our volume of $\frac{4}{3}\pi(150\text{Å})^3$. Room temperature bulk InSb seems to have calculated Auger lifetimes between 0.1 and 1 nanosecond, depending[70] on how the atomic orbitals and nonparabolic energy bands are calculated.

We are now studying processes affecting the dynamics of bound carriers in quantum dots. We have estimated rates of collisions of quantum dot carriers via the Coulomb interaction amd compared these rates to the competing interband and intraband radiative rates and phonon absorption/emission rates in quantum dots.

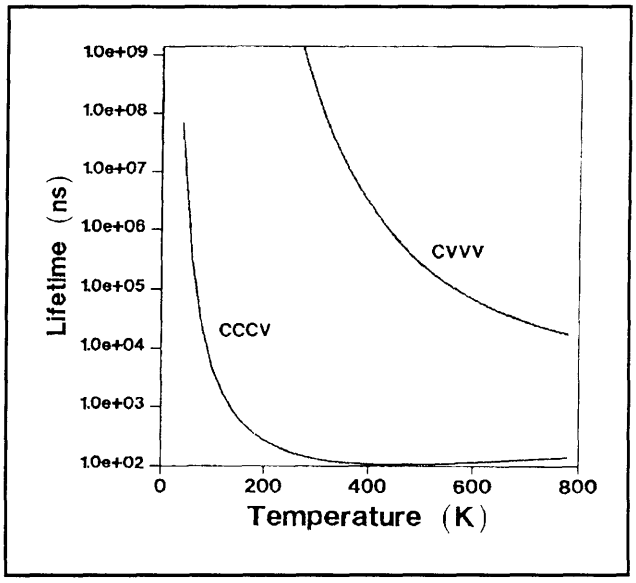

Figure 8. The temperature dependence of the CCCV and CVVV Auger lifetimes for a 150 Å radius InSb quantum dot surrounded by CdTe barriers. This is to be compared with the calculated Auger rates for other semiconductors with band gaps in the infrared.

---

66 G.P. Agrawal and N.K. Dutta, *Long Wavelength Semiconductor Lasers,* (New York: Van Nostrand Reinhold Co., 1986).

67 J.L. Pan, *Phys. Rev. B* 46: 3977 (1992).

68 A. Haug, D. Kerkhoff, and W. Lochmann, *Phys. Stat. Solid B* 89: 357 (1978).

69 R. Rosman and A. Katzir, *IEEE J. Quantum Electron.* QE-18: 814 (1982).

70 H. Bruhns and H. Kruse, *Phys. Stat. Solid B* 97: 125 (1980).

We are interested in materials and fabrication methods necessary for realistic devices. We have suggested various possibilities, such as InSb dots in CdTe barriers, in a recent paper.[71] Our long term goal is to fabricate and experimentally study quantum dots for use in lasers in the thermal infrared.

1.22 Coherent Fusion Theory

Project Staff

Professor Peter L. Hagelstein, Irfan U. Chaudhary, Akikazu Hashimoto, Sumanth Kaushik

Three and a half years have now passed since the announcement of the observation of anomalies in deuterated metals that was made in March 1989. Excess heat was reported by Pons and Fleischmann, and evidence for low level neutron emission was presented by Jones. Efforts to reproduce the effects were largely unsuccessful in 1989, and the scientific community has generally rejected these claims.

Pons and Fleischmann have continued their experiments, and their current claims are far more dramatic than those made in 1989. The initial 1989 reports described a relatively weak heat effect that was observed with relatively poor reproducibility; the claims of 1992 describe a very dominant effect that is completely reproducible, although still not understood.

At the Thirrd International Cold Fusion Conference in Nagoya, Japan, Pons and Fleischmann described reproducible observations of extreme excess heat production in electrolysis experiments, with a specific power generation rate of more than 3kW/cm^3 of Pd cathode.[72] This high level of heat production is sufficient to boil away the electrolyte (50 cc) completely in about 10 minutes. Energy production was monitored with their open-cell calorimeter, and gave a result that was consistent with an energy balance determination by multiplying the heat of vaporization of the electrolyte (about 41 kJ per mole) times the number of moles of electrolyte (2.5 moles), yielding about 100 kJ of energy output. The electrical energy input during this period was about 20 kJ, resulting in a power gain of about 4. The anomalous excess energy production during this period was close to 200 eV per atom of Pd.

We have continued to explore[73] theoretical mechanisms which could account for the heat anomaly, and for other anomalies (including tritium and ^{4}He production, and also gamma, neutron and fast ion emission) which continue to be reported by numerous laboratories.

We have considered several different types of possible nuclear reaction mechanism; fusion as a mechanism appears to be unlikely since there does not appear to be any practical way to get deuterium nuclei close enough to fuse at room temperature in a metal lattice. We have therefore proposed a new and speculative type of nuclear reaction involving the transfer of neutrons from "donor" nuclei to "acceptor" nuclei.

During the past year we have made progress towards understanding reactions in which a neutron is transfered from deuterium and then captured incoherently by a heavy metal nucleus, with no energy exchange with the lattice.[74]

---

[71] J.L. Pan, *Phys. Rev. B* 46: 3977 (1992).

[72] M. Fleischmann and S. Pons. "Calorimetry of the Pd-D_2O system: from Simplicity via Complications to Simplicity," *Proceedings of the Third Annual International Cold Fusion Conference,* Nagoya, Japan, November 1992.

[73] P.L. Hagelstein, "Coherent and Semi-Coherent Neutron Transfer Reactions I: The Interaction Hamiltonian," *Fusion Tech.* 22: 172 (1992); P.L. Hagelstein, "Coherent and Semi-Coherent Neutron Transfer Reactions II: Transition Operators," *Fusion Tech.* forthcoming; P.L. Hagelstein, "Coherent and Semi-Coherent Neutron Transfer Reactions III: Phonon Generation," *Fusion Tech.* 23: 353 (1993); P.L. Hagelstein, "Coherent and Semi-Coherent Neutron Transfer Reactions IV: Two-step Reactions and Virtual Neutrons," submitted to *Fusion Tech.*; P.L. Hagelstein, "Coherent and Semi-Coherent Neutron Transfer Reactions," *Proceedings of the Third Annual International Cold Fusion Conference,* Nagoya, Japan, November 1992.

[74] P.L. Hagelstein, "Coherent and Semi-Coherent Neutron Transfer Reactions IV: Two-step Reactions and Virtual Neutrons," submitted to *Fusion Tech.*; P.L. Hagelstein, "Coherent and Semi-Coherent Neutron Transfer Reactions," *Proceedings of the Third Annual International Cold Fusion Conference,* Nagoya, Japan, November 1992.

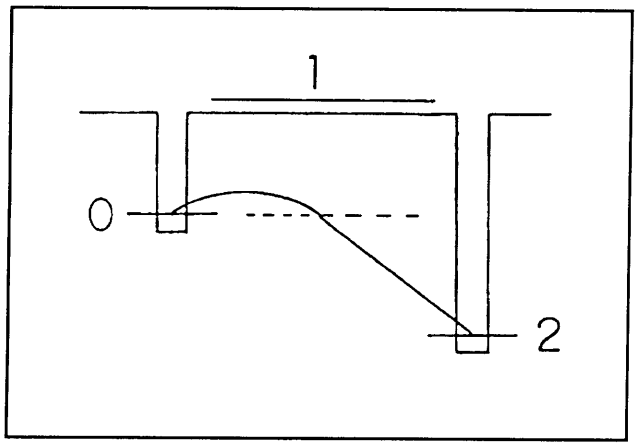

Figure 9. Schematic of a two-step reaction involving a virtual intermediate state.

This type of two-step reaction involves a virtual intermediate state that contains a free neutron. It is known that virtual neutrons in free space do not stray very far away from their point of origin. The Green's function for a virtual neutron in free space satisfies

$$[E - H_0]G(r|r_0) = \delta^3(r - r_0) \qquad (1)$$

In this case $H_0 = -\hbar^2\nabla^2/2M$, and the solution can be found analytically to be

$$G(r|r_0) = -\frac{1}{4\pi|r - r_0|}\frac{2M}{\hbar}\exp(-\alpha|r - r_0|) \qquad (2)$$

where $\alpha = \sqrt{2M|E|/\hbar^2}$ for E negative. The Green's function is damped exponentially, with a decay constant that is on the order of an inverse fermi. Because of this, one would naively expect that a virtual neutron would never be able to go as far as a neighboring nucleus.

We have explored the modifications in the virtual neutron Green's function that would be brought about by the presence of a periodic produced by a lattice. In this case, the Green's function satisfies

$$[E - H_0 - V(r)]G(r|r_0) = \delta^3(r - r_0) \qquad (3)$$

where the periodic potential *V(r)* is due to neighboring nuclei in the lattice. We have shown that the presence of the periodic potential gives rise to a long range component of the neutron Green's function. In the case of a weak perturbation, we have found a very accurate approximate result for the Green's function which exhibits explicitly long range effects that are on the scale of the characteristic Bragg extinction length (which can be on the order of a micron).

Unfortunately, the potential produced by nuclei in a lattice will normally be too weak to induce very much of an effect with being resonantly enhanced. Such a resonant effect has recently been identified: a virtual neutron that is transfered from a deuteron will be resonantly captured by a proton in an equivalent site to make another deuteron. By itself, this leads only to a weak correction of the Green's function; but if a rather specific type of phase correlation in space were to exist among the deuterons and protons in the lattice, then a rather dramatic enhancement of this new long range effect will take place.

We have conjectured that diffusion of hydrogen isotopes in the lattice would, in the quantum limit, produce the required coherence. Very recently we have obtained an existence proof of sorts that it is possible for a metal hydride to exhibit predominantly coherent tunneling near room temperature. It remains to be demonstrated that quantum diffusion produces Dicke states; this is an area of ongoing research.

One proposed model for heat production involves neutron transfer reactions in which the reaction energy is coupled into the lattice. In last year's RLE report we described an approach based on the Duschinsky operator which appears because the initial lattice phonon modes differ from the final state phonon modes due to the mass change at the site of the neutron transfer; the method proposed in that report was analyzed in detail and found to be incapable of significant energy transfer. It was found that the Duschinsky operator is not particularly efficient at creating phonons, but it appears to be capable of transfering energy through shifting the frequency of phonon modes.

Dilute impurities in a metal lattice can form reasonably precise phonon bands, termed impurity bands in the literature. If there are N_H interstitial hydrogen atoms and N_D interstitial deuterium atoms in a Pd lattice, then there will be $3N_H$ impurity modes at ω_H and $3N_D$ impurity modes at ω_D. If a neutron transfers off of a deuteron to make a proton, then the three highest deuterium impurity modes will be shifted to the hydrogen impurity band. The associated energy exhange with the lattice will be $n\hbar(\omega_H - \omega_D)$. Since the impurity band modes are true continuum modes, the number of phonons in a

single mode can be quite large, and the energy transfer can be anomalously large.[75]

The mechanism described above has the potential to couple energy even if the virtual neutron capture is incoherent. The anomalous energy transfer associated with neutron capture increases the energy available for possible nuclear reactions, which can increase the energy of reaction products and open new reaction channels. Such reactions may account for recent observations of copious emissions of gammas, alphas and neutrons from glow discharge experiments.[76]

1.23 Deuterated Metal Experiments

Sponsors

Space Exploration Associates
Future Energy Applied Technology, Inc.

Project Staff

Professor Peter L. Hagelstein, Professor Louis D. Smullin, D. Farber, Akikazu Hashimoto, Martin H. Muendel, Q. Zheng

If anomalous effects actually do occur in metal-deuterium systems, then it should be possible to develop experiments at MIT which demonstrate one or more of the anomalies. A controversy has existed since 1989 as to whether there exist any anomalous effects at all, with the large majority of the scientific community being currently in agreement that no new effects exist at all. The demonstration at MIT of one or more of the anomalies (excess heat production, tritium production, or energetic nuclear products) would be expected to impact this controversy.

A primary goal of our experimental effort is therefore to develop an experiment that demonstrates at least one anomalous effect, for the express purpose of placing research in this area into the mainstream of science.

The experimental results that have been obtained to date in other laboratories have not clarified what reaction mechanisms are involved in any positive sense. A major goal of the present effort is to work towards a basic understanding of the underlying reaction mechanism, and to provide experimental feedback for proposed theoretical mechanisms.

There are a number of experiments which have been done previously for which a confirmation at MIT would prove interesting. Additionally, there are new experiments that are motivated by theoretical considerations which could be attempted. The experimental program that we are currently pursuing includes both classes of experiment.

Our initial efforts towards developing experiments originated from theoretical ideas based on neutron transfer reaction model. As discussed above, the model is based on neutron transfers from donor nuclei (deuterium) to suitable acceptor nuclei. Heat production in the model follows from coherent neutron transfer from deuterium to lithium or boron; tritium production arises from coherent neutron capture on deuterium; gamma and alpha production follows from semi-coherent capture on metal nuclei; neutron and energetic ion emission would follow from neutron capture on nuclei accompanied by significant energy input from the lattice.

According to theory, significant relative phase coherence among pairs of interstitials in the lattice must be present before any anomalies can occur. For such relative phase coherence to be present, the interstitials must diffuse; the specifics of this process are under investigation theoretically. Metal deuterides are favored, since deuterium is the lightest interstitial that can donate a neutron. Palladium is favored since the diffusion coefficient of deuterium is one of the highest for an fcc lattice; but theory would suggest that V, Nb and Ta, which are bcc lattice and have lower diffusion barriers, may also prove interesting.

From theory, diffusion in the quantum limit will have the best chance of setting up the required phase coherence. A review of the experiments showing positive results indicate that most of them operate at temperatures somewhat (within a factor of 2) above where the diffusion is in the quantum limit. The faster the diffusion, the larger the coherence volume, hence the reactions should work better at higher temperatures up to a maximum temperature at which the phase differences accumulated between hydrogen and deuterium diffusion destroy the coherence. Where this occurs is unknown: the

---

[75] P.L. Hagelstein, "Coherent and Semi-Coherent Neutron Transfer Reactions III: Phonon Generation," *Fusion Tech.* 23:353 (1993).

[76] A.B. Karabut, Y.R. Kucherov, and I.B. Savvatimova, "Nuclear Product Ratio for Glow Discharge in Deuterium," *Phys. Lett. A* 170: 265 (1992).

early Karabut paper describes a cut-off at 500 K,[77] Fleischmann and Pons describe high heat generation with a temperature excursion up to about 600 K,[78] and Liaw reported excess heat in molten salt experiments near 700 K.[79] The solubility of Pd decreases markedly at higher temperature, which confuses the issue. In Nb, with higher solubility at elevated temperatures, effects have been reported at a temperature in excess of 1600 K.[80]

Consequently, higher temperature appears to be favorable for the anomalies. Inasmuch as this leads to delocalization of the metal interstitials and maintains relative phase coherence, it is consistent with theory.

The first experiments which we set out to explore involved tritium production. From a mechanistic point of view, tritium production is simpler than heat production since only light hydrogen interstitials are diffusing. The diffusion of heavier interstitials such as Li and B in PdD is not well understood, but it is clear that the associated diffusion coefficients will be smaller. Tritium production is mechanistically more complicated than semicoherent alpha or gamma production, since the lattice has to participate in a nontrivial way; going into the experiment we are not guaranteed that the lattice will be correctly excited to take up the reaction energy.

Observations of tritium production have been reported in numerous metal deuterides in a variety of electrochemical, gas loading, and glow discharge experiments. One such experiment was developed at LANL by Tom Claytor.[81] In this experiment, deuterium gas is absorbed by palladium that is part of a stack of alternating Si and Pd layers; a current is driven through the stack by pulses of high voltage. Tritium is reportedly produced under these conditions reproducibly at a rate of $10^6 - 10^7$ tritium atoms per second. Tritium production was also studied by Lanza, who assessed the relative rates for different metal host lattices.[82] Tritium production was reportedly observed in Ti, Zr, Hf, Ta, Ti-Zr and in Zircaloy 2; the highest production figures were found for Ta.

A gas ionization gauge has been developed that is capable of detecting ionizing radiation at low levels; this instrument is sufficiently sensitive to detect about 10^{10} tritium atoms, which would be produced in about 20 minutes of operation at a rate of 10^7 atoms/second (the maximum rate reported by Claytor).

The first experiments completed to date involved a search for tritium evolved from gas-loaded Ta using the ionization gauge as a tritium detector; no tritium was observed in this experiment. Follow-on experiments are planned that will test for tritium production in V, Nb, Ta, and Pd under conditions in which (1) it can be verified that the metal loaded; (2) current flow is present; and (3) increased temperatures are maintained.

One confirmation experiment that is planned is a replication of the Claytor experiment, to be carried out in collaboration with the LANL team. Recently, Claytor has reported success in producing tritium in a PdD_x wire loaded in deuterium gas driven by a pulsed current source. We are modifying our system to operate in this mode.

A second type of experiment that we have been developing is an attempt to obtain excess heat in a gas-loading experiment. The basic idea is to assemble donor (deuterium) and acceptor (boron) nuclei in a host metal lattice that is gas loaded and at high temperature. If successful, this type of system would be better adapted for potential applications than excess heat-producing electrochemical systems, both because it is technically simpler and because energy conversion from a high temperature source is more efficient.

---

[77] A.B. Karabut, Y.R. Kucherov, and I.B. Savvatimova, "Nuclear Reactions at the Cathode in a Gas Discharge," *Sov. Tech. Phys. Lett.* 16: 463 (1990).

[78] M. Fleischmann and S. Pons, "Calorimetry of the Pd – D_2O System: from Simplicity via Complications to Simplicity," *Proceedings of the Third Annual International Cold Fusion Conference,* Nagoya, Japan, November 1992.

[79] B.Y. Liaw, P.-L. Tao, P. Turner and B.E. Liebert, "Elevated-temperature Excess Heat Production on a Pd + D Dystem," *J. Electroanal. Chem.* 319: 161 (1991).

[80] V.A. Romodanov, V.I. Savin, and Y.M. Timofeev, "Nuclear Fusion in Condensed Matter," LUTCH report UDC:539.172.13; presented at the *Third Annual International Cold Fusion Conference,* Nagoya, Japan, November 1992.

[81] T.N. Claytor, D.G. Tuggle, and H.O. Menlove, "Evolution of Tritium from Palladium in the Solid State Gas Cell," presented at the *Third Annual International Cold Fusion Conference,* Nagoya, Japan, November 1992.

[82] F. Lanza, G. Bertolini, V. Vocino, E. Parnisari, and C. Ronsecco, "Tritium Production Resulting from Deuteration of Different Metals and Alloys," *Proceedings of the Second Annual Cold Fusion Conference* 151 (1991).

An experiment has been constructed to carry out this type of experiment. It consists of a heater that is surrounded by a deuterium gas filled annulus in which the metal sample is held and monitored. The central heater and annulus are surrounded by magnesium oxide thermally resistant bricks; due to the general appearance of the resulting structure, it has earned the moniker "Lenin's Tomb." As a calorimeter, Lenin's Tomb has been calibrated and has been found to be reproducible from day-to-day while heating; power excesses on the order of a watt would be detectable. In the initial trial runs of undoped vanadium (no boron) in deuterium, no excess heat has been observed to date.

From theory, gamma and alpha emission due to semi-coherent neutron capture on metal nuclei should occur as a precursor and during coherent reactions. This is of interest since the fully coherent reactions are difficult to diagnose unless they work at high levels. From a theoretical point of view, the semi-coherent reactions are simpler since they do not require any special degree of lattice excitation.

We have used a NaI gamma detector to search for excess gamma emission from gas loaded vanadium in Lenin's Tomb, as a signature of precursor activity. The background is very high, and no positive signals were identifiable.

A next step in the experiment is to arrange for current flow in the deuterated metal samples, and to diagnose for gamma emission in V, Nb, Ta and Pd. Some effort needs to be put into improving the signal to noise ratio in the gamma detection. The positive observation of a precursor signal would be a significant step forward experimentally, and would bode well for possible observations of an excess power anomaly. Experiments on boron-implanted gas loaded metals constitute the next phase of the experiments.

We had worked for about a year on the experiments described above when we learned of some closely related glow-discharge experiments that were reported at the International Cold Fusion Conference in Nagoya last November. In these experiments, various metals were loaded by glow discharge at high temperature and anomalies were observed. One group at the LUTCH Association in Moscow observed gammas, alphas and neutrons at very high levels $10^5 - 10^6$ per second in glow discharge experiments using a Pd cathode; very high levels of excess power (more than 1 kilowatt/cm^3) were also observed.[83] Another experiment at LUTCH used a similar glow discharge to study tritium production at high temperature in a variety of metals; tritium production at the very high rate of 1.7×10^9 atoms/second was observed in Nb at 1170 K.[84] Glow discharge experiments in China gave intense neutron and gamma signals from a variety of metals, including Pt, Nb, W and Pd.[85]

These experiments are closely related in that metal deuterides at high temperature exhibit positive precursor signals, as well as heat and tritium production. They differ from the experiments that we have been developing in that the cathodes are actively loaded by the discharge and achieve very high D/Pd loading ratios, and also that substantial current density is present in the cathodes. We decided to attempt a confirmation of one of the glow discharge experiments performed at LUTCH.

We have developed a glow discharge that runs under conditions similar to those reported by the LUTCH group, in terms of operating current, voltage and gas pressure. This discharge is unusual in that the cathode surface current density can reach several hundred milliamps/cm^2; this high surface current level is accompanied by high cathode temperatures which appears to be important. This experiment will be carried out in collaboration with Y. Kucherov of the LUTCH group.

---

[83] A.B. Karabut, Y.R. Kucherov, and I.B. Savvatimova, "Nuclear Product Ratio for Glow Discharge in Deuterium," *Phys. Lett. A* 170: 265 (1992).

[84] V.A. Romodanov, V.I. Savin, and Y.M. Timofeev, "Nuclear Fusion in Condensed Matter," LUTCH report UDC:539.172.13; presented at the *Third Annual International Cold Fusion Conference,* Nagoya, Japan, November 1992.

[85] L. Heqing et al., presented at the *Third Annual International Cold Fusion Conference,* Nagoya, Japan, November 1992.